



**TRIBHUVAN UNIVERSITY  
INSTITUTE OF ENGINEERING  
PULCHOWK CAMPUS**

**THESIS NO: 2073/MSMS/855**

**THE EFFECT OF GRID ELECTRODE STRUCTURE AND SURFACE AREA  
OF ELECTRODE ON PERFORMANCE OF ALKALINE WATER  
ELECTROLYSIS**

**By**

**Dharmdev Yadav**

**A THESIS**

**SUBMITTED TO THE DEPARTMENT OF APPLIED SCIENCES AND  
CHEMICAL ENGINEERING**

**IN PARTIAL FULFILLMENT OF THE REQUIREMENTS FOR THE  
DEGREE OF MASTER OF MATERIALS SCIENCE AND ENGINEERING**

**DEPARTMENT OF APPLIED SCIENCES AND CHEMICAL ENGINEERING**

**PULCHOWK, LALITPUR, NEPAL**

**February, 2021**

## RECOMMENDATION



It is certified that Mr. Dharmdev Yadav has carried out the thesis work entitled “**THE EFFECT OF GRID ELECTRODE STRUCTURE AND SURFACE AREA OF ELECTRODE ON PERFORMANCE OF ALKALINE WATER ELECTROLYSIS**” under my Supervision. I recommended the thesis in the partial fulfillment for the requirement of Master’s Degree of Materials Science and Engineering.

---

Supervisor Prof. Dr. Shankar Pd. Shrestha  
Department of physics, Patan Multiple Campus,  
Tribhuvan University, Patandhoka,  
Lalitpur, Nepal

## **COPYRIGHT**

The author has agreed that the library, Department of Applied Sciences and Chemical Engineering, Pulchowk Campus, Institute of Engineering may make this thesis freely available for inspection. Moreover, the author has agreed that permission for extensive copying of this thesis for scholarly purpose may be granted by the professor(s) who supervised the work recorded herein or, in their absence, by the Head of the Department wherein the thesis was done.

It is understood that the recognition will be given to the author of this thesis and to the Department of Applied Sciences and Chemical Engineering, Pulchowk Campus, and Institute of Engineering in any use of the material of the thesis. Copying or publication or the other use of this thesis report for financial gain without approval of the Department of Applied Sciences and Chemical Engineering, Pulchowk Campus, Institute of Engineering and author's written permission is prohibited. Request for permission to copy or to make any other use of this thesis in whole or in part should be addressed to:

Head

Department of Applied Sciences and Chemical Engineering

Pulchowk Campus, Institute of Engineering

Lalitpur, Kathmandu

Nepal

**TRIBHUWAN UNIVERSITY**  
**INSTITUTE OF ENGINEERING**  
**PULCHOWK CAMPUS**  
**DEPARTMENT OF APPLIED SCIENCES AND CHEMICAL ENGINEERING**

The undersigned certify that they have read, and recommended to the Institute of Engineering for acceptance, a thesis entitled "The effect of Grid Surface and Surface area of electrode on performance of alkaline water electrolysis" submitted by Dharmdev Yadav in partial fulfillment of the requirements for the degree of Master in Materials Science and Engineering.

---

Supervisor, Prof. Dr. Shankar Shrestha

Department of Physics, Patan Multiple Campus, Patandhoka Lalitpur, Tribhuvan  
University

---

External Examiner, Prof. Dr. Bhadra Prasad Pokharel

Department of Applied Sciences and Chemical Engineering, IOE, Pulchowk, Tribhuvan  
University

---

Committee Chairperson, Prof. Dr. Ram Kumar Sharma

Head of the Department, Department of Applied Sciences and Chemical Engineering,  
IOE, Pulchowk, Tribhuvan University

Date: February, 2021

## EVALUATION



We certify that we have read this thesis and in our notion, it is an excellent work the scope and quality as thesis in the partial fulfillment for the requirement of Master's Degree of Materials Science and Engineering.

---

Supervisor

Prof. Dr. Shankar Pd. Shrestha, Department of Physics,

Patan Multiple Campus, Patandhoka, Lalitpur, Tribhuvan University, Nepal

---

## ABSTRACT

The electrolysis cell is constructed to study I-V characteristic of electrodes with electrolyte (1M NaOH). In addition, current verses input power ( $P_{in}$ ) and resistance verses voltage curve of the cell is also study, at difference fixed grid voltage. The I-V Characteristic of electrodes show reaction is not started (that is not current observed) at low applied voltage but with increasing the voltage reaction started linearly for both small and large grid window size.

The input power for both small and large grid window increase linearly. The resistance of cell goes decrease with grid voltage increase, decrease with increase grid voltage and become constant with increase grid voltage for anode, cathode and grid electrodes respectively for both windows. Moreover the excremental observed value for hydrogen production is higher than theoretical value, which is an error but minimum for both windows.

The efficiency of hydrogen with the help of current and voltage at different electrodes are about 68%. This may be due to the concentration of electrolyte, nature of electrode materials and system constructed. With increase the surface area of grid electrode then increase the hydrogen production rate. This is because large surface area goes to contact with large number of electrolyte molecules and the production of hydrogen depend up on this contact i.e. larger surface area has large number of reaction. Therefore the productions of hydrogen gas depend upon the surface area of grid. Grid voltage increases and cathode current  $I_c$  is also increases with input power  $p_{in}$ . Thus, in general one can say with increasing the grid voltage cell resistance decrease. The resistance of cell decrease sharply in between 0.5V to 1.0V with grid voltage while seen almost constant beyond 3.5V.

**Keywords:** Electrolyte, Electrodes, Power, Hydrogen, grid windows etc.

## **ACKNOWLEDGEMENT**

This research is an outcome of support and co-operation of many individual and organization. I am very thankful to supervisor, Prof. Dr. Shankar Prasad Shrestha, who provided insight and expertise that greatly assisted the research. I am very grateful for the support of Prof. Dr. Bhadra Prasad Pokharel, Program Coordinator of Master in Materials Science and Chemical Engineering.

I would like to thank Department of Physics, Patan Campus. I own great amount of gratitude to the Department of Applied Sciences and Chemical Engineering at Pulchowk Campus, Institute of Engineering, and Tribhuvan University for supporting in the research conducted. I am grateful towards my classmates and peers for sharing their wisdom with me during the course of this research.

I would like to express our profound gratitude towards Pulchowk Campus, Patan Multiple Campus, Trichandra Multiple Campus, and Innovative Ghar Nepal for their co-operation and providing necessary arrangement of using laboratory equipment's regarding the thesis. Our thanks and appreciations also go to our department teachers, campus staff, friends and colleagues in developing the thesis and people who have helped to me, with their abilities.

I am very grateful for endless love, support and trust from my parents, which carried me till here. Last but not the least; I would like to thank all those who have directly or indirectly helped me throughout this thesis.

## TABLE OF CONTENTS

<b>RECOMMENDATION</b> .....	<b>1</b>
<b>COPYRIGHT</b> .....	<b>2</b>
<b>EVALUATION</b> .....	<b>4</b>
<b>ABSTRACT</b> .....	<b>5</b>
<b>ACKNOWLEDGEMENT</b> .....	<b>6</b>
<b>LIST OF FIGURES</b> .....	<b>10</b>
<b>LIST OF TABLES</b> .....	<b>12</b>
<b>LIST OF SYMBOLS</b> .....	<b>13</b>
<b>LIST OF ACRONYMS AND ABBREVIATIONS</b> .....	<b>14</b>
<b>CHAPTER ONE: INTRODUCTION</b> .....	<b>15</b>
1.1 Background .....	15
1.2 Electrolysis of water .....	15
1.3. Factor affecting Electrolysis.....	16
1.4Applications of Water Electrolysis .....	17
1.5Working Principle .....	18
1.5.1 Chemical Reaction .....	19
1.6I-V Characteristics Curve .....	20
1.7Objectives .....	21
<b>CHAPTER TWO: LITERATURE REVIEW</b> .....	<b>22</b>
2.1 History of Electrolysis .....	23
2.2 Efficiency of hydrogen production with electrode current.....	26



2.3. Hydrogen production and utilization .....	27
<b>CHAPTER THREE: RESEARCH METHODOLOGY.....</b>	<b>30</b>
3.1 Experimental Methodology .....	30
3.2 Experimental apparatus .....	30
3.2.1 Construction of electrolytic cell.....	30
3.2.2 Electrodes.....	31
3.2.3 Grid.....	32
3.2.4 One mole of NaOH solution .....	33
3.2.4 Burette .....	33
3.2.5 Fixing nuts and bolts .....	33
3.3 Experimental setup .....	34
3.4 Computational Methodology .....	34
3.5. Experimental Methods .....	35
<b>CHAPTER FOUR: RESULTS AND DISCUSSION.....</b>	<b>37</b>
4.1 Results .....	37
4.2 I-V Characteristics of Electrolyzer with Small Window Size Grid Electrode.....	37
4.2.1 Effect of $V_g$ on $I_a$ Verse $V_{ca}$ Curve .....	38
4.2.2 Effect of $V_g$ on $I_c$ Verse $V_{ca}$ Curve .....	40
4.2.3 Effect of $V_g$ on $I_g$ verse $V_{ca}$ curve.....	43
4.2.4 Effect of $V_g$ on Input power ( $P_{in}$ ) verse Cathode Current ( $I_c$ ) Curve .....	44
4.3 I-V Characteristics of Electrolyzer with Large Window Size Grid Electrode.....	45
4.3.1 Effect of $V_g$ on $I_a$ verse $V_{ca}$ Curve .....	46

4.3.2 Effect of $V_g$ on $I_c$ Verse $V_{ca}$ Curve .....	48
4.3.3 Effect of $V_g$ on $I_g$ verse $V_{ca}$ Curve .....	50
4.3.4 Effect of $V_{ca}$ on Input Power ( $P_{in}$ ) verse Cathode Current ( $I_c$ ) .....	51
4.4. The Comparison Graph between Small & Large Window Size Grid Electrode at Grid Voltage $V_g=3.0V$ .....	53
4.5. Comparison Graph of experimental and Theoretical ( $H_2$ ) Production rate verse Current .....	53
4.6. Comparison of Pin with cathode current at constant grid voltage .....	54
<b>CHAPTER FIVE: CONCLUSION .....</b>	<b>55</b>
5.1 Conclusion.....	55
5.2 Future work.....	55
<b>References .....</b>	<b>56</b>
<b>Appendix.....</b>	<b>60</b>

## LIST OF FIGURES

Figure 1.1: Electrolysis of water .....	18
Figure 1.2: I-V Curve .....	20
Figure 3.1: Simple voltammetry cell and Electrolyzer .....	31
Figure 3.2: Electrodes .....	32
Figure 3.3: Grid electrode (Steel jail) .....	32
Figure 3.4: Fixing nuts and bolts .....	33
Figure 3.5: Circuit Diagram of experiment to observed data for thesis work.....	35
Figure 4.1: power supply connection for three electrode electrolyzer in common cathode configuration.....	37
Figure 4.2.: the variation of anode current ( $I_a$ ) Verse applied voltage ( $V_{ca}$ ) for the cell with small window size grid.....	39
Figure 4.3: Graph showing variation of cell resistance ( $R$ ) with grid voltage ( $V_g$ ) of Table 4.1.....	40
Figure 4.4: The variation of cathode current ( $I_c$ ) Verse applied voltage ( $V_{ca}$ ) for the cell with small window grid.....	41
Figure 4.5: Graph showing variation of cell resistance ( $R$ ) with grid voltage ( $V_g$ ) of Table 4.2.....	42
Figure 4.6: The variation of cathode current ( $I_c$ ) Verse applied voltage ( $V_{ca}$ ) for the cell with small windows size grid.....	43
Figure 4.7: Graph showing variation of cell resistance ( $R$ ) with grid voltage ( $V_g$ ) of Table 4.3.....	44
Figure 4.8: Plot of cathode current ( $I_c$ ) verse input power ( $P_{in}$ ) at different fixed grid voltage ( $V_g$ ) for common grid cell electrode configuration.....	45
Figure 4.9: the variation of anode current ( $I_a$ ) Verse applied voltage ( $V_{ca}$ ) for the cell with large window size grid.....	46
Figure 4.10: Graph showing variation of cell resistance ( $R$ ) with grid voltage ( $V_g$ ) of Table 4.4.....	47

Figure 4.11: the variation of cathode current ( $I_c$ ) Verse applied voltage ( $V_{ca}$ ) for the cell with large window grid.....	48
Figure 4.12: Graph showing variation of cell resistance (R) with grid voltage ( $V_g$ ) of Table 4.5.....	49
Figure 4.13: Variation of cathode current ( $I_c$ ) Verse applied voltage ( $V_{ca}$ ) for the cell with large windows size grid .....	50
Figure 4.14: Graph showing variation of cell resistance (R) with grid voltage ( $V_g$ ) of Table 4.6.....	51
Figure 4.15 Plot of cathode current ( $I_c$ ) verse input power ( $P_{in}$ ) at different fixed grid voltage ( $V_g$ ) for common grid cell electrode configuration.....	52
Figure 4.16: The comparison graph between small & large window size grid electrode at grid voltage $V_g=3.0V$ .....	53
Figure 4.17: Plot of hydrogen production rate verse current at different fixed grid voltage ( $V_g$ ) for common grid cell electrode configuration.....	54
Figure 4.18: Figure 4.18: Input Power vs cathode current with large and small windows sizes.....	54
Figure A1: Power Supply 1 Vs Standard Multimeter voltage.....	61
Figure A2: Power Supply 2 Vs Standard Multimeter voltage.....	61

## LIST OF TABLES

Table 4.1: Reaction starting voltage, over potential, slope and operating resistance of the cell for anode current at different fixed grid voltage.....	39
Table 4.2: Reaction starting voltage, over potential, slope and operating resistance of the cell for anode cathode ( $I_c$ ) at different fixed grid voltage.....	42
Table 4.3: Reaction starting voltage, over potential, slope and operating resistance of the cell for grid current at different fixed grid voltage.....	44
Table 4.4: Reaction starting voltage, over potential, slope and operating resistance of the cell for anode current at different fixed grid voltage.....	47
Table 4.5: Reaction starting voltage, over potential, slope and operating resistance of the cell for anode cathode ( $I_c$ ) at different fixed grid voltage.....	49
Table 4.6: Reaction starting voltage, over potential, slope and operating resistance of the cell for grid current at different fixed grid voltage.....	51
Table 4.7: Hydrogen and Oxygen Production rate.....	53

## LIST OF SYMBOLS

°	Degree
%	Percentage
KOH	Potassium hydroxide
ml	Milliliter
N	Normality
M	Morality
NaOH	Sodium hydroxide
H <sub>2</sub>	Hydrogen Gas
O <sub>2</sub>	Oxygen Gas
H <sub>2</sub> O	Water
<b>Δ</b>	Delta
<b>Ω</b>	Resistance
A	Current
V	Voltage
W	Watt

## LIST OF ACRONYMS AND ABBREVIATIONS

AC	Alternative Current
DC	Direct Current
PEM	Proton Exchange Membrane
$I_c$	Cathode current
$I_a$	Anode current
$I_g$	Grid current
$V_g$	Grid voltage
$V_{ca}$	Anode to cathode voltage
$V_g$	Grid voltage
$P_{in}$	Input Power
R	Resistance

## CHAPTER ONE: INTRODUCTION

### 1.1 Background

Water electrolysis is the promising option for Hydrogen Production from renewable energy. Water electrolysis is the process of splitting water into the Hydrogen and Oxygen gas for electricity. Water electrolysis technology was much more flexible and tenable solution to store renewable energy on a large, long-term scale. Using excess renewable electricity the Proton Exchange Membrane (PEM) electrolyzer splits water into its constituent parts, hydrogen and oxygen, that can be stored in common tanks. Hydrogen production by electrolysis water is dependent on the factor that directly affects the efficiency of Hydrogen production (Bouazizi Nabil, 2014).

We have studied the increase the rating of hydrogen generators to meet the demand of the growing renewable power industry in Nepal as well as others also.(Rosen, 2008) The renewable energy was enhanced through the use of hydrogen energy system in which is hydrogen is the one type of energy carrier. The world energy sources become less fossil fuel-based; hydrogen and electricity are expected to be the two dominant energy carriers for the provision of end-use services, in a hydrogen economy. Many researchers in their work have done for analyzing the energy consumption, efficiency of hydrogen production system.(M.M, k, H, & M, 2015)Thus, hydrogen energy systems allow greater use of renewable energy resources.

### 1.2 Electrolysis of water

Electrolysis of water is the decomposition of water ( $H_2O$ ) into oxygen ( $O_2$ ) and hydrogen gas ( $H_2$ ) due to an electric current being passed through the water. The reaction has a standard potential of  $-1.23V$ , meaning it ideally requires a potential difference of 1.23 volts to split water. The technique can be used to make hydrogen fuel (hydrogen gas) and breathable oxygen, though currently most industrial methods make hydrogen fuel from natural gas(A.F.M, 2011).

Research results show that the temperature, pressure, electrode material, electrolyte formulation and concentration, physical setup of the cell and power supply output waveform have an influence on the value of over potential.



According to Faraday's law of electrolysis that "the local gas mass flow rate is proportional to the local current density" .i.e., "the mass of substance produced at an electrode during electrolysis is proportional to the number of moles of electrons transferred at the electrode". Hence, the goal of an energy efficient water electrolysis process is to reach higher level of the current while applying the minimum possible voltage to the electrode. Most available literatures, discussions on this subject are based on the physical and chemical configuration of electrolytic bath rather than its electric properties.

### **1.3. Factor affecting Electrolysis**

Factors affecting efficiency of water electrolysis such as the electrolyte type, electrodes spacing, electrodes surface morphology (smooth or rough), electrodes effective area (or number of electrodes) and electrodes connection configuration were investigated. The efficiency was calculated as the ratio between the HHO flowsrates measured experimentally to that measured theoretically from Faraday's law. It is found that the best efficient electrolyzer consists of 22 plates (4 anodes, 4 cathodes and 14 neutrals) where each plate area was  $17 \times 15 \text{ cm}^2$ . When the 22 plates were connected in parallel and immersed in 20 g KOH/3L electrolyte, they produced HHO gas flow rate of 740 ml/min at 17 A and 62.92 % efficiency (Kandah, 2014).

(Galney, 2009) studied the electrolysis process efficiency of a high temperature and pressure electrolyte. He found that an acceptable fall in the amount of required voltage in the case of targeting any given current density is achieved at atmospheric pressure and temperature levels between  $200^\circ\text{C}$  and  $400^\circ\text{C}$ . On the other hand, (Nagi et al. 2003) expressed that conducting electrolysis in higher temperature decrease the equilibrium voltage of water because it enlarges the gas bubbles size and reduces their rising velocity. As a result, the void fraction in the electrolyte will increase and the efficiency will decrease.

(Mansouri et al. 2001) tried to increase the efficiency and lower the capital costs of hydrogen production by reaching higher current density in the conventional electrolyzers. They found that increasing electrolyte pressure leads to less power consumption as it reduces the diameter of produced gas bubbles. Therefore, the ohmic voltage drop and power dissipation between electrodes are reduced. (Badwal et al. 2006) found that the pH

of the water that is used as the electrolyte affected the required voltage to drive an electrolytic bath on a certain current significantly due to the conductivity of the electrolyte. On the other hand, it is well known that high acid or base concentration liquids have severe negative corrosion effects on the electrodes. Therefore, a balance between the pH and voltage is required.

(Petrov et al. 2011) found that 25-30% KOH solution is the most suitable concentration in the electrolysis processes. (Mazloomi and Nasri, 2012) have analyzed several factors influencing water electrolysis efficiency by studying available verified information in electrical, electrochemical, chemical, thermodynamics and fluid mechanics fields such as distance between electrodes, their size, alignment and shape.

#### **1.4 Applications of Water Electrolysis**

The atmosphere is polluted by plenty of greenhouse gases; SO<sub>x</sub>, NO<sub>x</sub>, CO<sub>2</sub>, and CO from hydrogen production by hydrocarbon source that are fossil fuel sources which can affect seriously the ecosystem. Hence the clean technology is needed for production of hydrogen that can be achieved if hydrogen is produced by renewable source like water electrolysis and no emission of SO<sub>x</sub>, NO<sub>x</sub>, CO<sub>2</sub>, and CO will be possible and to achieve “hydrogen economy”(Y. Petrov, 2011). There are many important non-fossil fuel based processes like Water electrolysis, photo catalysis processes and thermo chemical cycles for hydrogen productions in practice(W.P., 2004).

Hydrogen based energy system are known as promising replacements for conventional technologies. Water electrolysis meanwhile is known to be one of the important assets for hydrogen production(H.P. & A.K., 1979).

Enhancing the efficiency of the water electrolysis is thus of considerable practical interest, as electricity expenses make up a large part of hydrogen production costs. The required voltage value of an electrolysis cell is higher than the decomposition voltage of a water molecule. The excess voltage is known as over potential of the cell. Numerous scientific entities over the world have put on much effort to reduce the over potential(P.Millet, 2010).

Electrolysis of water is the decomposition of water (H<sub>2</sub>O) into oxygen and hydrogen gases when electricity is passed through it. This technique can be used to make hydrogen

fuel and breathable oxygen, though currently most industrial methods make hydrogen fuel from natural gas.

The (Santos, 2013) hydrogen produced by renewable energy sources. It has the main advantage of mobility. It is essential for supplying energy in remote areas away from the main electricity grid like Hydropower.

(Voitic, 2018)Hydrogen Production utilization and Temperature should be inversely proposal to energy. Thus it is the highest interest for the future hydrogen economy to raise this percent of efficiency and reduce the hydrogen production price(V.M. Nikolic, 2010).

### 1.5 Working Principle

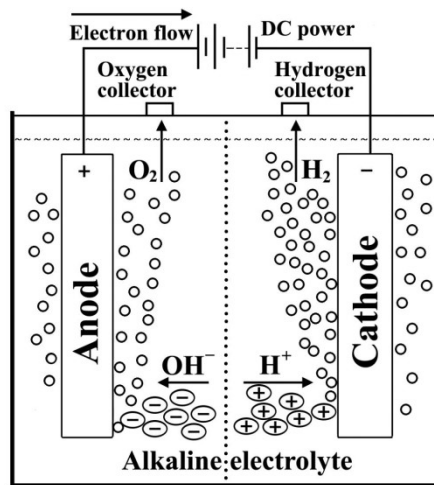


Figure 1.1: Electrolysis of water

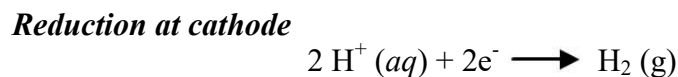
A DC electrical power source is connected to two electrodes, or two plates (typically made from inert metal such as platinum, stainless steel or iridium) which are placed in the water. Hydrogen will appear at the cathode (the negative electrode, where electrons enter the water), and oxygen will appear at the anode (the positive electrode). Assuming ideal faradic efficiency, the amount of hydrogen generated is twice the amount of oxygen, and both are proportional to the electrical charge conducted by the solution. However, in many electrodes competing side reactions occur, resulting in different products and less than ideal faradic efficiency.

Electrolysis of *pure* water requires excess energy in the form of over potential to overcome various activation barriers. Without the excess energy the electrolysis of pure

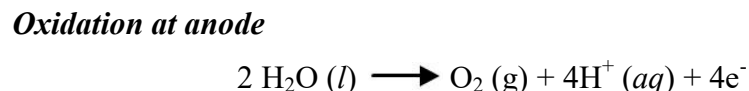
water occurs very slowly or not at all. This is in part due to the limited self-ionization of water. Pure water has an electrical conductivity about one millionth that of sea water. Many electrolytic cells may also lack the requisite electro catalysts. The efficiency of electrolysis is increased through the addition of an electrolyte (such as a salt, an acid or a base) and the use of electro catalysts.

### 1.5.1 Chemical Reaction

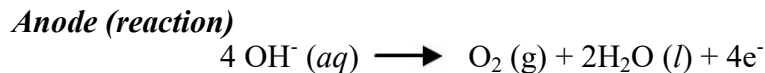
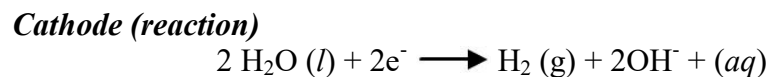
In pure water at the negatively charged cathode, a reduction reaction takes place, with electrons ( $e^-$ ) from the cathode being given to hydrogen cations to form hydrogen gas (the half reaction balanced with acid): (Passas and Dunhill)



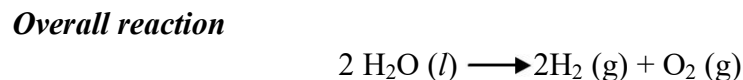
At the positively charged anode, an oxidation reaction occurs, generating oxygen gas and giving electrons to the anode to complete the circuit:



The same half reactions can also be balanced with base as listed below. Not all half reactions must be balanced with acid or base. Many do, like the oxidation or reduction of water listed here. To add half reactions they must both be balanced with either acid or base.



*Combining either half reaction half reaction pair yields the same overall decomposition of water into oxygen and hydrogen:*



The number of hydrogen molecules produced is thus twice the number of oxygen molecules. Assuming equal temperature and pressure for both gases, the produced hydrogen gas has therefore twice the volume of the produced oxygen gas. The number of electrons pushed through the water is twice the generated oxygen molecules.

### 1.6I-V Characteristics Curve

The water electrolysis performance is normally evaluated with the current voltage characteristics of an electrolytic cell as shown in figure below. Several models have been developed to try to simply and effectively simulate the current voltage characteristics of PEM electrolysis for hydrogen production. To evaluate water electrolysis in hydrogen production, a concise model was developed to analyze the current voltage characteristics of an electrolytic cell.

This model describes the water electrolysis capability by means of incorporating thermodynamic and electrical resistance effects. These two effects are quantitatively expressed with two main parameters; the thermodynamic parameter which is the water disassociation potential; and the ohmic parameter which reflects the total resistance of the electrolytic cells with various operating conditions can be conveniently compared with each other.

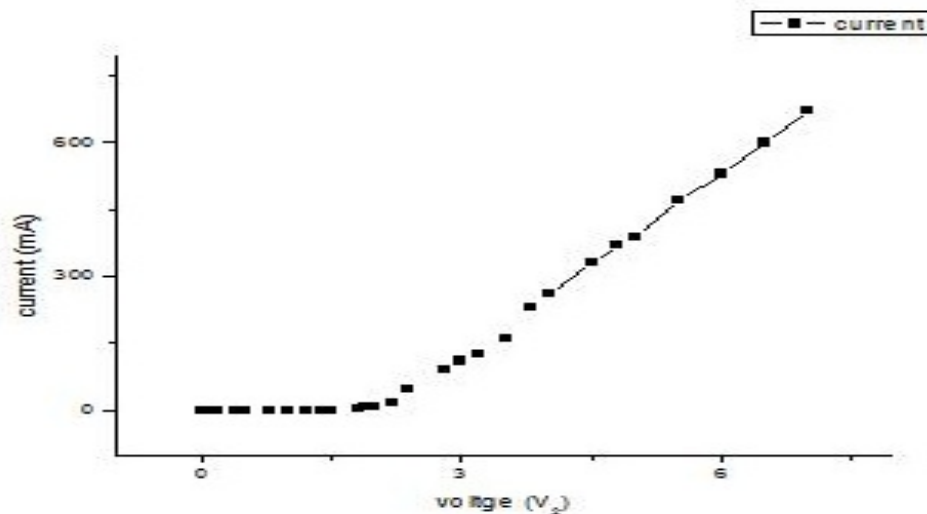


Figure 1.2: I-V Curve

$V_{\min}$ : The minimum voltage value of the IV curve also yields information as to the efficiency of the cell. A low  $V_{\min}$  implies a higher efficiency process. (Walch, 2014)

lowest of the (V) possible theoretical value should be 1.23 V, corresponding to the potential for water splitting in reality no gas evolution is observed below 1.65 to 1.7 V, hence there is a need for the over potential. The  $V_{\min}$  was accessed by extrapolation of the straight line part of the graph to  $I = 0$  value and is effectively the voltage at which the cell begins to operate as water splitting device rather than a capacitor, when the minimum over potential has been achieved.

### **1.7 Objectives**

The main principle objectives of the work are:

- ✓ To study the electrolysis of water by placing steel grid electrode of large and small window size in between anode and cathode.
- ✓ To study the hydrogen production rate by using large and small windows size in grids electrode.
- ✓ To study the calibration of two DC power supply, three multimeter with standard multimeter.
- ✓ To study the efficiency of hydrogen production rate with large and small windows size.

## CHAPTER TWO: LITERATURE REVIEW

Today the electrolysis process has been recognized as the most important method to generate hydrogen ( $H_2$ ) for many power applications owing to their performance. Moreover, the hydrogen is identified as an upcoming fuel for a viable energy supply. The renewable energy source such as wind and solar thermal energy can be adopted to obtain hydrogen from electrolysis process. An increase in future demand for hydrogen is depending on the increasing demand for energy in both transportation and stationary applications.

Nevertheless, the global energy demand has been increasing rapidly. Consequently, the traditional energy sources such as coal, gas and liquefied petrol are being reduced at an alarming rate. This problem could be solved by using renewable energy sources as a backup energy supply. These days the generation of hydrogen from the electrolysis process has become one of most useful renewable energy technology in the world.

Water electrolysis systems offer several advantages over traditional technologies including higher energy efficiency, higher production rates, and more compact design. Electrolytes, potassium hydroxide (KOH), and sulfuric acid ( $H_2SO_4$ ) are used to in the experiments, the voltage and current were measured. The concentration of the electrolyte significantly affected the electrolyser performance. Overall the best case was with 15 wt%  $H_2SO_4$  at the anode channel and 20 wt% at the cathode channel with. In addition, increasing the difference in concentration of the sulfuric acid had an effect on the diffusion. The diffusion flux became larger when the difference in concentration became larger, increasing electrolyser efficiency without the addition of extra energy (Sun and Hsiau, 2018).

The catalytic properties of phosphate species, already shown on the reduction reaction in anaerobic corrosion of steels, are exploited here for hydrogen production. Phosphate species work as a homogeneous catalyst that enhances the cathodic current at mild pH values. A voltammetric study of the hydrogen evolution reaction is performed using phosphate solutions at different concentrations on 316L stainless steel and platinum rotating disk electrodes. Hydrogen is produced in an electrolytic cell using a phosphate

solution as the catholyte. Results show that 316L stainless steel electrodes have a stable behavior as cathodes in the electrolysis of phosphate solutions. Phosphate (1 M, pH 4.0/5.0) as the catholyte can equal the performance of a KOH 25%w solution with the advantage of working at mild pH values. The use of phosphate and other weak acids as catalysts of the hydrogen evolution reaction could be a promising technology in the development of electrolysis units that work at mild pH values with low-cost electrodes and construction materials (Munoz et al., 2010).

## **2.1 History of Electrolysis**

From the discovery of the phenomenon of electrolytic splitting of water into hydrogen and oxygen to the development of modern electrolyzers, water electrolysis technology has seen continuous progresses over the past 200 years(Zeng and Zhang, 2010).

Following the discovery of electricity, J.R. Deiman and A.P. van Troostwijk, in 1789, used an electrostatic generator to discharge electricity through two gold wires placed inside a tube filled with water, causing evolution of gases(Levie, 1999).

Alessandro Volta invented the voltaic pile in 1800, and a few weeks later William Nicholson and Anthony Carlisle used it for electrolytic splitting of water(Kreuter and Hofmann, 1998). Later, the gases produced during water electrolysis were identified to be hydrogen and oxygen. With the development of electrochemistry, the proportional relationship between electrical energy consumption and the amount of gases produced became established through Faraday's law of electrolysis. Finally, the concept of water electrolysis was defined scientifically and acknowledged(Riegar, 1987).

With the invention of the Gramme machine in 1869 by Zénobe Gramme, water electrolysis became an economical method of producing hydrogen. A technique for industrial synthesis of hydrogen and oxygen through water electrolysis was developed later in 1888 by Dmitry Lachinov. By 1902, more than 400 industrial water electrolyzers were already in operation. The period between the 1920s and the 1970s was the “golden age” for the development of water electrolysis technology, when most of the traditional designs were created.

Driven by the industrial need for hydrogen and oxygen, the knowledge established in the first stage was applied to the industrialization of water electrolysis technologies. In 1939, the first large water electrolysis plant, with a capacity of  $10,000 \text{ Nm}^3\text{H}_2\text{h}^{-1}$ , went



into operation, and in 1948, the first pressurized industrial electrolyzer was manufactured by Zdansky/Lonza. Commercial water electrolysis concepts developed in this period include most of the technological components that are currently in use (Bowen et al., 1984).

One of these components is the membrane. The first membranes to be commercialized were made of asbestos. However, asbestos is not very resistant to corrosion caused by a strongly alkaline environment at high temperatures. Moreover, due to its seriously adverse health effects, asbestos was gradually replaced by other materials. From the 1970s onward, polymers based on perfluorosulfonic acid, arylene ether, or polytetrafluoroethylene have been used as gas separation material (Rosa et al., 1995 and Hickner, et al., 2004). Configuration of the water electrolysis cell also underwent several improvements through time. Typical conventional tank cells, with a unipolar configuration, are simple, reliable, and flexible.

On the other hand, filter press cells, with a bipolar configuration, have lower Ohmic losses and are more compact. High-pressure water electrolyzers, which use the bipolar configuration, would be difficult to accomplish with unipolar cells. Disadvantages of the bipolar cells are related to their structural complexity, requirement of electrolyte circulation, and use of gas/electrolyte separators (Divisek et al., 1990 and Sequeira and Santos, 2010). The electrode material selected should have good corrosion resistance, high conductivity, high catalytic effect, and low price (Wendt and Kreysa, 1999).

Stainless steel and lead were pointed out as cheap electrode materials, with low overpotentials, but these cannot tolerate highly alkaline environments. Noble metals were found to be too expensive to be used as bulk electrode materials. Ni was then recognized as an electroactive cathode material with good corrosion resistance in an alkaline solution (when compared to other transition metals) and rapidly became popular during the development of water electrolyzers. Ni-based alloys have then started to be the object of extensive research efforts (Bocca et al., 1998).

These progresses motivated commercialization of water electrolyzers. The first records of commercial water electrolysis date back to 1900, when the technique was still in its early life. Two decades later, large-size electrolysis plants, rated at 100 MW, were developed in Canada, primarily to feed the ammonia fertilizer industries. In the late

1980s, Aswan installed 144 electrolyzers with a nominal rating of 162 MW and a hydrogen generation capacity of  $32,400 \text{ m}^3 \text{ h}^{-1}$ . The Brown Boveri electrolyzer is another highly modularized unit, which is able to produce hydrogen at a rate of about  $4300 \text{ m}^3 \text{ h}^{-1}$ . Stuart Cell (Canada) is a well-known unipolar tank-type cell manufacturer.

Hamilton Sundstrand (USA), Proton Energy Systems (USA), Shinko Pantec (Japan), and Wellman-CJB (UK) manufacture the latest proton exchange membrane (PEM) electrolyzers. In the first half of the 20th century, there was a huge demand for hydrogen in the production of ammonia fertilizers. This need for hydrogen stimulated the development of water electrolysis technology, which was helped by the low cost of hydroelectricity at the time. However, then hydrocarbon energy started to be applied massively in industry.

Hydrogen could be produced in large scale through coal gasification and natural gas reforming, and at much lower costs, gradually fading the economic advantage of water electrolysis. At that point, progresses on water electrolysis for hydrogen production simply ceased. The oil crisis of the 1970s renewed the worldwide interest in water electrolysis.<sup>1</sup> In the new hydrogen economy ideology, hydrogen was being considered to be the energy carrier of the future and the key to solve the problem of sustainable energy supply. Improving the efficiency of water electrolysis became a major goal.

Novel breakthroughs were achieved at the cell level, with the emergence of PEM and pressurized water electrolyzers. Compact, high-pressure water electrolyzers were used to produce oxygen on board the nuclear-powered submarines, as part of the life-supporting system. The compact design eliminates the gaskets between cells, requiring high-precision machining of the cell frames. However, high operating pressures of these water electrolyzers (up to 3.5 MPa) create a major safety problem.<sup>1</sup> In 1966, General Electric for the first time used a Nafion membrane to supply energy for space projects.

However, special requirements are needed for several of its components (e.g., expensive polymer electrolyte membrane, porous electrodes, and current collectors), which are its serious disadvantages. Currently, many efforts are under way to integrate renewable energy technologies as energy sources in water electrolysis for hydrogen production, as a means for distributed energy production, storage, and use, particularly in

remote communities. New water electrolysis concepts, such as photovoltaic (PV) electrolysis and steam electrolysis, are now emerging (Pletcher and Walsh, 1990).

Ming-Yuan Lin, 2012 In 1800 Alessandro Volta invented the voltaic pile, and a few weeks later William Nicholson and Anthony Carlisle used it for the electrolysis of water. When Zenobe Gramme invented the Gramme machine in 1869 electrolysis of water became a cheap method for the production of hydrogen (M. & K.F, 1989). A method of industrial synthesis of hydrogen and oxygen through electrolysis was developed by Dmitry Lachinov in 1888.

In 1875, Dr. Charles Michel, invented an experiment with ways to remove the painful ingrown eyelashes of his patients. The early techniques used fine wires attached to a battery to produce galvanic electrolysis. This was a chemical method that utilized direct current to convert normal body salt and water into the compound sodium hydroxide (lye). Lye destroys the cells that initiate hair growth. The galvanic electrolysis method is still used today, although the modern mechanics are now much more efficient and computerized.

In 1923, after the discovery of radio waves and high frequency current, a new method of electrolysis was born. This method, called thermolysis, uses high frequency current to produce heat. The heat cauterizes and destroys the cells in the follicle that cause hair growth.

Nowadays, Clean Energy is need of this world while the world generating lots of pollutants enough to change adversely the ecosystem (K. & D, 2010). In Ref. by A. Ursa, stand-alone operation of an alkaline water electrolyser fed by wind and photovoltaic systems is studied. In that analysis study, it was investigated that the electrolyser is performed properly, with regard to balance of plant and its principal electrochemical characteristics. Moreover, the mean energy efficiency of the electrolyser was found for each wind and PV system.

## **2.2 Efficiency of hydrogen production with electrode current**

In water electrolysis, (Lin, 2012) the Hydrogen production in the cathode for a certain amount of electrical power input is lower than the theoretical value. To gain a certain amount of hydrogen output, the actual electrical power needed will be more than the theoretical one. Due to the resistances in the electrolytic solution and electrodes caused

by side reactions, inverse reactions, and impurity of electrode materials, the current efficiency is always less than 100%. In water electrolysis, hydrogen production is proportional to the electric current.

Present days, (Eedulakanti, 2019) energy storage and storage systems i.e. batteries, fuel cells, electrochemical capacitors and solar cells, are currently under intensive research and development

(Prinith, 2019) The concentration of surfactants also has an impact on electrocatalytic action on electro active species and studied. There are different types of water electrolysis in which water is splits into hydrogen and oxygen. There are three types of electrolysis: electrolysis, thermolysis and photo electrolysis(Dunnill, 2015).

### **2.3. Hydrogen production and utilization**

About 113.2 million metric tons of hydrogen was produced in 2017 in the world (McWilliams, 2019). Approximate market value was 115.25 billion USD in 2017. This market is expected to grow to 154.74 billion USD in 2022(Valladares, 2017). Hydrogen can be produced from various sources such as, water, natural gas, oil, biomass and (after gasification) from coal (Turner, 2004). Globally, 95 % of hydrogen is produced from fossil fuels. Nowadays, hydrogen is mainly produced from natural gas via steam methane reforming, although partial oxidation of oil and gasification of coal are also used. Electrolysis (mainly alkaline electrolysis) method has a minor role in hydrogen production

The estimated total hydrogen production in Finland is 200,000 t/a. Corresponding shares by technology are 86 % steam methane reforming, by-product (electrolysis) 11 %, partial oxidation of heavy fuel 2 % and water electrolysis 1 %. The largest share of the hydrogen is produced at Neste Oil Kilpilahti refinery (around 120,000 t/a). The biggest water electrolysis plant (alkaline) with capacity of 1300 t/a is at Woikoski in Kokkola Industrial park (Hurskainen and karki, 2018 and Kauranen et al., 2013). Today, the primary uses of hydrogen are in the chemical industry. Ammonia and fertilizer production 51 %, and in oil refining industry 31 %. Noteworthy 11 % of the produced hydrogen is processed into methanol. Other chemicals, processing and steel, glass,

welding sectors account for a minor part of the hydrogen consumption (Hydrogen Council, 2017).

Hydrogen consumption in Finland is dominated by oil refining 82 %. Chemical industry, mainly consisting of hydrogen peroxide ( $H_2O_2$ ) and hydrochloric acid (HCl) production, is second largest sector with 7 % along with heat and electricity sector 6 %. The vented hydrogen 2 % comes from the chlorine/chlorate electrolysis plants. Hydrogen consumption is expected to rise. Annual demand could increase from about 8EJ to almost 80EJ by 2050. This increase would be due to rise in hydrogen use in industrial, residential, transportation and power sectors. The corresponding reduction potential of  $CO_2$  is 6 Gt annually. For this scenario to happen, policy and financial support with notable cost reductions are mandatory (IRENA, 2018).

Ideally, 39 kWh of electricity and 8.9 liters of water are required to produce 1 kg of hydrogen at 25°C and 1 atmosphere pressure. Typical commercial electrolyzer system efficiencies are 56%–73% and this corresponds to 70.1–53.4 kWh/kg (NREL, 2004). Two basic types of low temperature electrolyzers alkaline and proton exchange membrane are currently being manufactured.

The first water electrolyzers used the tank design and an alkaline electrolyte. These electrolyzers can be configured as unipolar (tank) or bipolar (filter press) designs. In the unipolar design, electrodes, anodes, and cathodes are alternatively suspended in a tank that is filled with a 20%–30% solution of electrolyte (potassium hydroxide in pure water). In this design, each cell is connected in parallel and operated at 1.9–2.5V<sub>dc</sub>. The advantage to this design is that it is extremely simple to manufacture and repair. The disadvantage is that it usually operates at lower current densities and lower temperatures (Konopka and Gregory, 1975). More recent unipolar designs include operation at high hydrogen pressure outputs (up to 6,000 psig).

The bipolar design, often called the filter-press, has alternating layers of electrodes and separation diaphragms that are clamped together. The cells are connected in series and result in higher stack voltages. Since the cells are relatively thin, the overall stack can be considerably smaller than the unipolar design. The advantages to the bipolar design are the reduced stack footprints, higher current densities, and its ability to produce higher

pressure gas. The disadvantage is that it cannot be repaired without servicing the entire stack (Kincaide, 1978). Fortunately, it rarely needs servicing. Previously asbestos was used as a separation diaphragm, but manufacturers have replaced or are planning to replace this with new polymer materials such as Ryton (Ryton, 2006).

## **CHAPTER THREE: RESEARCH METHODOLOGY**

### **3.1 Experimental Methodology**

We have using several methods of electrolysis and new ideas of cell designing, various research works has been conducted throughout the world for improvement of cell or (electrolyzer) efficiency. Therefore, we have also designed the new version of cell device which is designed the new concept and the concept name is “Third electrode system”. We have used in third electrode as steel grid electrode. In this chapter three, we have included all the experimental and computational researched methods that we were carried out in laboratory during research. The procedure and methods carried during the research methods are explained as systematically below.

### **3.2 Experimental apparatus**

We have used the experimental apparatus in this research work is steel mesh, steel electrode or steel plate electrode, multimeter, Two DC power supply, water measuring equipment, Burret, conical flask, digital weight machine, sodium hydroxide (NaOH) and polymer cuboidal cell. The polymer obtained from local market was used in this research or thesis work. Steel plate was used as electrode for electrolysis of water. There are three multimeter are used and obtained from local market and there are two DC Power suppliers are also obtained from local market. The Burret, Burret stand, measuring cylinder and digital weight machine are obtained from Lab.

#### **3.2.1 Construction of electrolytic cell**

The cuboidal shape of two polymer of dimension  $10\text{cm}\times 9.8\text{cm}\times 1.8\text{cm}$  is drilled into square shape of dimension  $5\text{cm}\times 5\text{cm}\times 1.8\text{cm}$ . The drilled area is filled with electrolyte solution (NaOH solution). Two holes are made diagonally at the upper part of each polymer for insertion of plastic pipes of diameter 0.5cm. The holes are designed for the gas out. At the lower, side part of one polymer is drilled to make a hole for the injection of electrolyte solution. Overall, there are five holes of same diameter. The length of plastic pipes is fixed such that the levels of electrolyte must be same level on all five pipes.

The grid (steel plate) divides whole electrolytic space into two equal parts where one mole solution of NaOH is stored. The outer part of the two polymer cell is now closed by steel plate (cathode and anode electrode) of dimension 10.4cm×9.7cm×0.1cm. These steel plates are fixed by nuts and bolt using rigid wooden pieces. Wooden pieces are used to prevent our electrolyzer from short circuit.

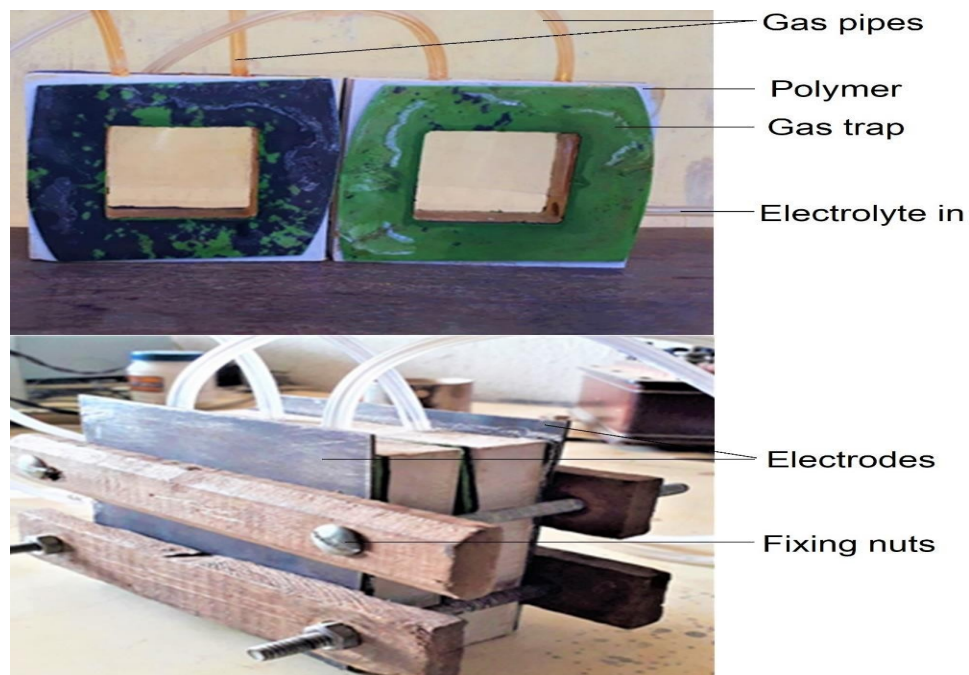


Figure 3.1: Simple voltammetry cell and Electrolyzer

### 3.2.2 Electrodes

The main factor that affects the efficiency of the cell is electrode materials that used in the electrolysis process. The most of the electrodes used are graphite, platinum, aluminum, nickel, iron, cobalt, gold etc. but in our case, we used steel plates as electrode that is anode, cathode and grid electrodes. The steel plates have the dimension 10.8cm ×9.8cm ×0.1cm and the steel plates used in our experiment.



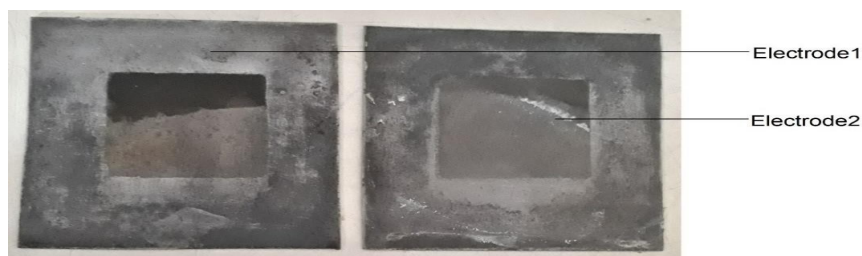


Figure 3.2: Electrodes

### 3.2.3 Grid

We have used the third electrode as the common steel grid electrode. The grid electrode is placed in between anode and cathode electrode. In our experiment carried out using a grid made up of steel which is placed in between the electrodes and 4cm distant from the electrodes. A jumper wire connected in the grid to measure the grid current.



Figure 3.3: Grid electrode (Steel jail)

### 3.2.4 One mole of NaOH solution

Molarity is defining as the number of moles of a solute per liter of solution. One mole of NaOH contained 40 gm of NaOH. By dissolving 40 gm of NaOH in 1000ml of distilled water we get one mole of NaOH solution as our electrolyte.

### 3.2.4 Burette

A volumetric burette is used to measure the volume of liquid. In our experiment we used two burettes of 50 ml. It is observed that, Hydrogen gas is collected at cathode side where as Oxygen gas is collected at anode side as expected theoretically. The  $H_2$  and  $O_2$  gas are collected in the ratio of 2:1. Thus with the help of burette we can easily find the volume of gases yield from electrolysis of water.

### 3.2.5 Fixing nuts and bolts

Electrolyzer is now fixed by four identical nuts and bolts using four rectangular rigid wooden pieces of length 15cm as shown in Figure 3.4. Here we use wooden pieces to prevent our device from short circuit.



Figure 3.4: Fixing nuts and bolts

### 3.3 Experimental setup

The experimental cell device is constructed on the basis of new ideas of cell construction and the cell device as shown in figure 3.1 and the inner volume of cell device is nearly 100 cm whereas electrolytic solution of normal water is subjected. In our experiment, we have used to 1 mole of NaOH electrolytic solution with normal water. The electrolytic solution is passed through the pipe connected to the lower side hole of the polymer until the level of electrolytic solution on all the five pipes is maintained.

There are four pipes  $P_1$ ,  $P_2$ ,  $P_3$  and  $P_4$  at the upper roof of the cell are connect with the two 600 ml. In experimental arrangement for the alkaline water electrolysis in our laboratory. We have used the two identical power suppliers (BAKUBK-1502DD) and three multimeters (one DT830D for cathode current  $I_c$ , one DT830D for anode current  $I_a$  and one DT830D for grid current). The circuit diagram of our experiment is as shown in figure. Here, the negative terminal of the power supply ( $P_1$ ) is connected to the electrode which acts as cathode electrode and positive terminal of same power supply ( $P_1$ ) is connected to electrode 2 which acts as anode electrode.

Similarly, the positive terminal of the power supply ( $P_2$ ) is connected to the electrode 3 which acts as grid electrode and the negative terminal of same power supply ( $P_2$ ) is connected to the common junction of power supply ( $P_1$ ). For the I-V characteristics, the data of current flow through the electrodes is taken at the different fixed grid voltage ( $V_g$ ) and the graph for the I-V curve is plotted with the help of the origin pro programming and the data are taken until the result is reproduced. Similarly, the curve characteristics for power input versus current at different electrodes can also be plotted with the use of origin software

### 3.4 Computational Methodology

- The Origin Program is used to plot the graphical data.
- The collected data are inscribed in this software.
- Then, the graph is plotted between voltage and current.

- The graph is plotted between input power and cathode current
- The graph is plotted between grid voltage and resistance value

### 3.5. Experimental Methods

A DC voltage is surmounted with the help of two DC power supplies according to the given circuit. Hydrogen forms on the cathode, while oxygen forms on the anode. The grid voltage is kept constant throughout around some certain values ( $V_g = 0.5V, 1.0V, 1.5V, 2V, 2.5V, 3V, 3.5V, 4V$ ) and actual voltage is varied from 0.1 to 10 volt. The voltmeter and ammeter readings are taken with the help of digital multimeters.

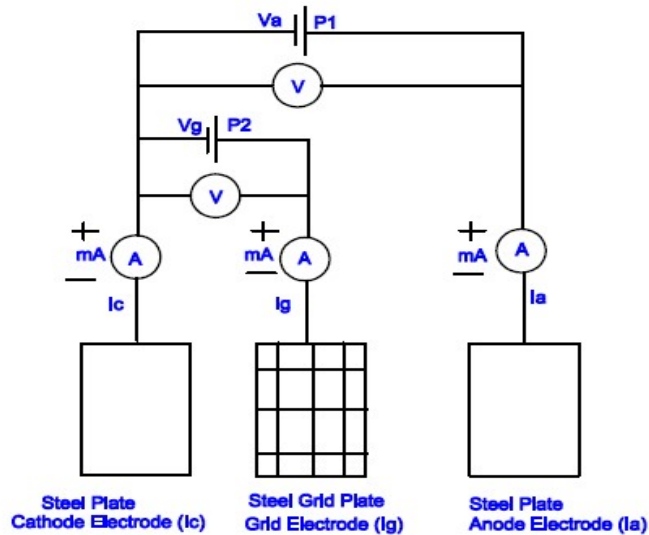


Figure 3.5: Circuit Diagram with common grid electrode configuration

The circuit diagram of our experiment is as shown in figure. Here, the negative terminal of the power supply ( $P_1$ ) is connected to the electrode 1 which acts as cathode electrode and positive terminal of same power supply ( $P_1$ ) is connected to electrode 2 which acts as anode electrode. Similarly, the positive terminal of the power supply ( $P_2$ ) is connected to the electrode 3 which acts as grid electrode and the negative terminal of same power supply ( $P_2$ ) is connected to the common junction of power supply ( $P_1$ ).

For the I-V characteristics, the data of current flow through the electrodes is

taken at the different fixed grid voltage ( $V_g$ ) and the graph for the I-V curve is plotted with the help of the origin pro programming and the data are taken until the result is reproduced. Similarly, the curve characteristics for power input versus current at different electrodes can also be plotted with the use of origin software.

A basic electrolyte 1M NaOH is used because OH<sup>-</sup> is non-poison and the gas production is pure and accurate. But if we used acidic electrolyte the estimation of hydrogen production measurement is inaccurate because acid itself contains hydrogen ions which combined with other ions to form hydrogen gases. The grid electrode is placed in between the anode and cathode at about 2cm from anode and cathode.

## CHAPTER FOUR: RESULTS AND DISCUSSION

### 4.1 Results

The electrolysis cell is constructed using two cuboidal polymers and a steel mesh grid is placed in between two electrodes. For the study of electrolysis of water, the concentration of electrolyte (1M NaOH) is used in the cell. The I-V characteristic is study by observing the data. In addition, current verses input power ( $P_{in}$ ) and resistance verses voltage curve of the cell is study. To study this, grid voltage ( $V_g$ ) is fixed at 0.5V, 1.0V, 1.5V, 2.0V, 2.5V, 3.0V, 3.5V and 4.0V. The current across cathode, anode and grid are observed with the help of ammeter. The observed data are analysis using origin software shown below in different subsection.

### 4.2 I-V Characteristics of Electrolyzer with Small Window Size Grid Electrode

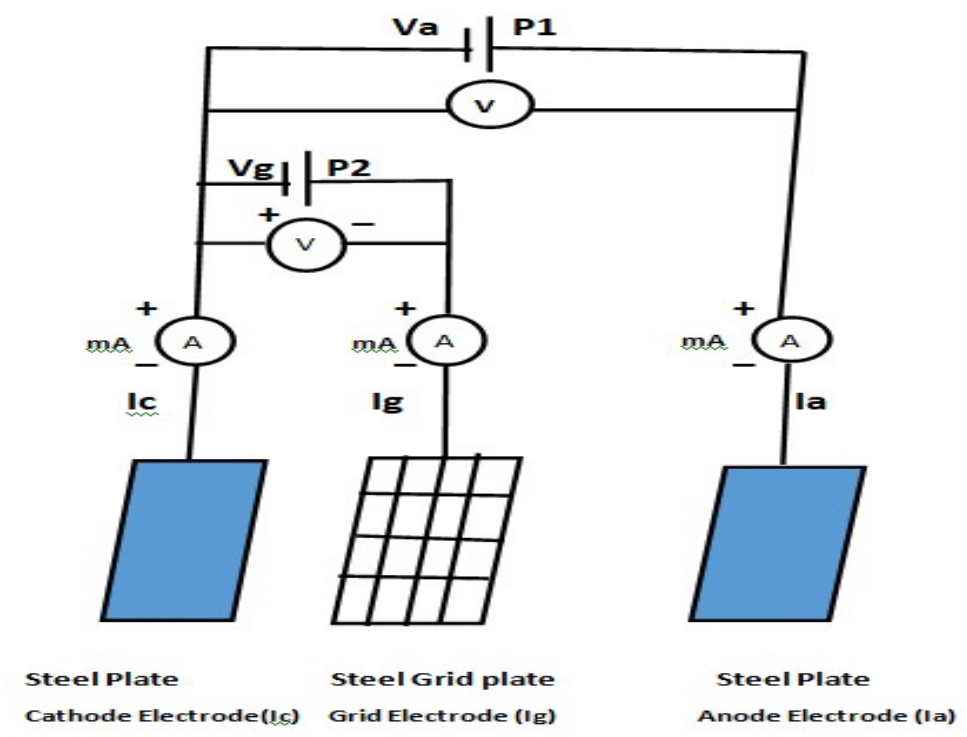


Figure 4.1: Power supply connection for three electrode electrolyzer in common cathode configuration.

Above, figure 4.1 shows that the circuit diagrams for power connection for the common cathode electrode configuration for alkaline water electrolyzer. Here steel mesh is used as

grid electrode and placed in between anode electrode and cathode electrode. In this case, small window size steel mesh is used for grid electrode. In this figure 4.1, negative terminal of power supply ( $P_1$ ) is connected to the cathode electrode ( $I_c$ ) and positive terminal of power supply ( $P_1$ ) is connected to the anode electrode.

Similarly, the positive terminal of power supply ( $P_2$ ) is connected to the grid electrode and negative terminal to the common junction of power supply ( $P_1$ ) and power supply ( $P_2$ ). The potential difference between anode electrode and cathode electrode is anode and cathode potential difference ( $V_{ca}$ ). Using 1 mole solution of (NaOH) electrolyte solution and data has been recorded for fixed grid voltage. We have measured the anode current ( $I_a$ ), grid current ( $I_g$ ) and cathode current ( $I_c$ ) by varying  $V_{ca}$  for different fixed voltage ( $V_g$ )

#### 4.2.1 Effect of $V_g$ on $I_a$ Verse $V_{ca}$ Curve

Figure 4.2 shows that the curve of anode current ( $I_a$ ) with applied voltage ( $V_{ca}$ ) at different fixed grid voltages at 0.5V, 1.0V, 1.5V, 2.0V, 2.5V, 3.0V, 3.5V and 4.0V. From the graph, we find that, at grid voltage ( $V_g$ ) = 0.5V case, as applied voltage ( $V_{ca}$ ) is increased from 0 to 1.7 volts, no anode current is observed. Anode current ( $I_a$ ) appears to start when as applied voltage ( $V_{ca}$ ) is greater than 1.7V which indicates the starting voltage for water electrolysis.

Beyond 1.7V the anode current ( $I_a$ ) increases linearly. From graph, we obtained as applied voltage ( $V_{ca}$ ) increases and anode current ( $I_a$ ) also increases linearly. Theoretical water splits to start at 1.23V, which is considered as threshold voltage for water electrolysis. In our case, at  $V_g=0.5V$ , the reaction starting voltage is found to be 1.8V and over potential is 0.57V. The reaction starting voltage, over potential, slope and cell resistance is tabulated in 2<sup>nd</sup>, 3<sup>rd</sup>, 4<sup>th</sup> and 5<sup>th</sup> columns of table 4.1 respectively. The slope of the curve for different fixed grid voltages are determined by the linear fitting of curve.

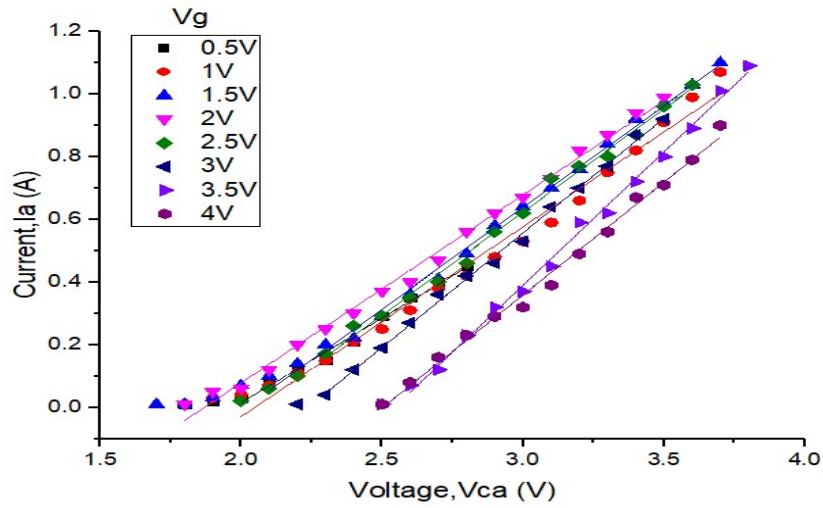


Figure 4.2.: The variation of anode current ( $I_a$ ) Verse applied voltage ( $V_{ca}$ ) for the cell with small window size grid

Table 4.1: Reaction starting voltage, over potential, slope and operating resistance of the cell for anode current at different fixed grid voltage

Fixed grid voltage( $V_g$ ) in volt	Reaction starting voltage ( $V_s$ ) in volt	Over potential in volt( $V_s - 1.23$ )	Slope of the curve	Resistance(1/slope) in ohm
0.5	1.8	0.57	0.54	1.85
1	2	0.77	0.62	1.61
1.5	2	0.77	0.62	1.61
2	2	0.77	0.623	1.61
2.5	2	0.77	0.65	1.54
3	2.2	0.97	0.73	1.37
3.5	2.5	1.27	0.85	1.32
4	2.7	1.47	0.87	1.29



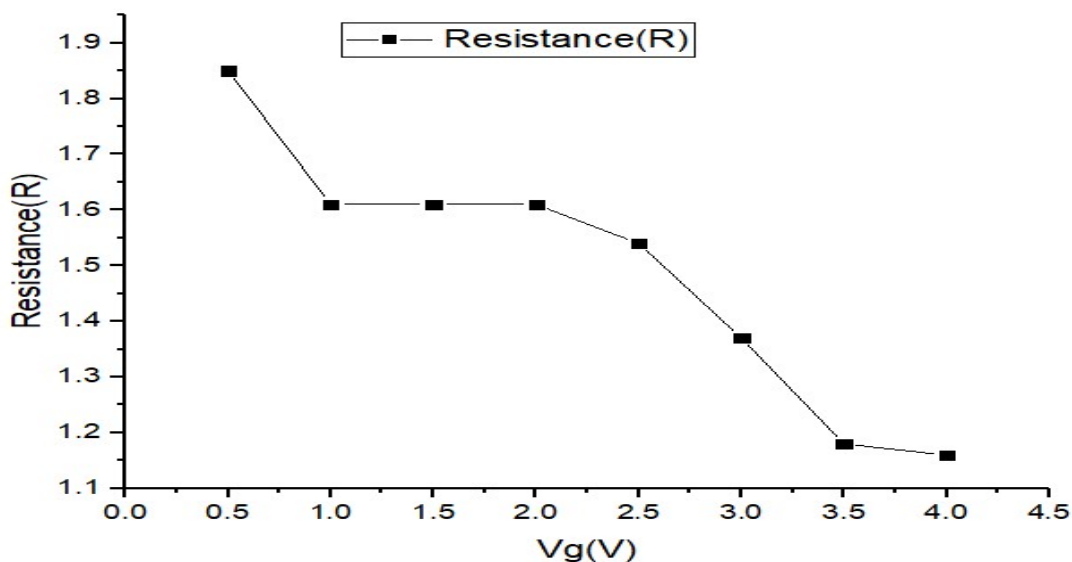


Figure 4.3: Graph showing variation of cell resistance (R) with grid voltage ( $V_g$ ) of Table 4.1

From above Figure 4.3 show that the variation of cell resistance (R) with grid voltage ( $V_g$ ). The plot for fixed grid voltage at  $V_g=0.5V$ , the resistance was observed 1.85ohm; at  $V_g=1.0V$ , the resistance was observed 1.61ohm; at  $V_g=1.5$ , the resistance was observed 1.61ohm and so on. The graph above shown in figure 4.3 shows high resistance (1.85ohm) at low grid voltage (0.5V). On increasing grid voltage the cell resistance decreases with slope. Thus, in general one can say with increasing the grid voltage cell resistance decrease. The resistance of cell decrease sharply in between 0.5V to 1.0V with grid voltage while seen almost constant beyond 3.5V.

#### 4.2.2 Effect of $V_g$ on $I_c$ Verse $V_{ca}$ Curve

Figure 4.4 shows that the curve of cathode current ( $I_c$ ) with applied anode voltage ( $V_{ca}$ ) with fixed grid voltages 0.5V, 1.0V, 1.5V, 2.0V, 2.5V, 3.0V, 3.5V and 4.0V. The graph from figure 4.4. Shows at  $V_g=0.5V$  the reaction starting voltage above the 1.8V and then we observed  $V_{ca}$  is increases and  $I_c$  is also increases linearly. At  $V_g=2.0V$  the cathode current ( $I_c=0.1A$ ) and applied voltage ( $V_{ca}$ ) are constant up to 1.9V then the reaction starting voltage above 2V then cathode current increases and applied voltage increases linearly.

At  $V_g=2.5V$  the cathode current ( $I_c=0.2A$ ) and applied voltage ( $V_{ca}$ ) are constant up to 1.9V then the reaction starting voltage above 2V then cathode current increases and applied voltage increases linearly and similar nature is observed for other grid voltage. The reaction starting voltage, over potential, slope and resistance is tabulated in 2<sup>nd</sup>, 3<sup>rd</sup>, 4<sup>th</sup> and 5<sup>th</sup> columns of table 4.2 respectively. The slope of the curve for different fixed grid voltage is determined by the linear fitting of curve.

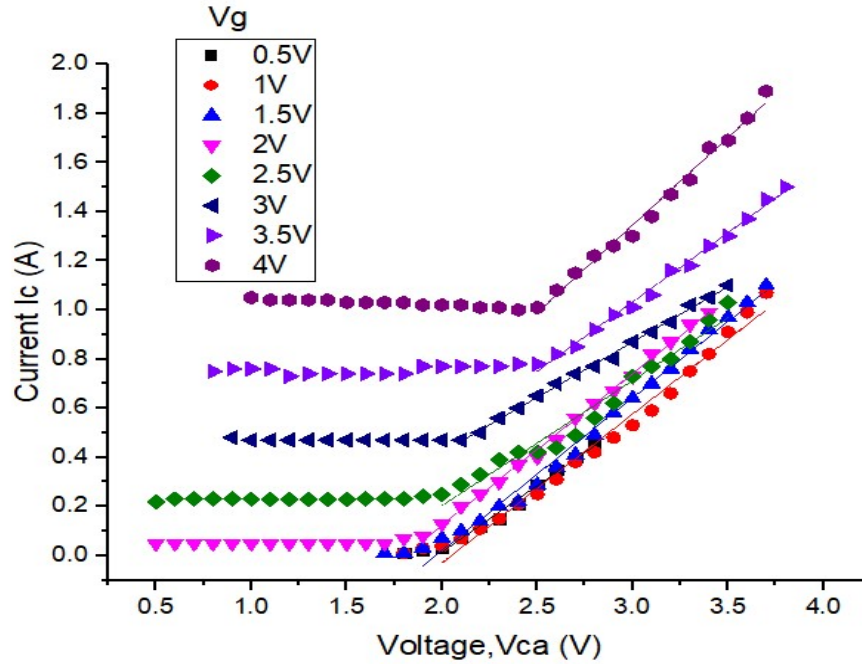


Figure 4.4: The variation of cathode current ( $I_c$ ) Verse applied voltage ( $V_{ca}$ ) for the cell with small window grid.

The cathode current is minimum or tends to zero because the threshold potential required for the reaction is 1.23 and grid voltage can't cross this threshold potential although grid voltage increase up to 2V. This is because impurities and concentration of electrolyte and experimental arrangement. With increasing grid and applied voltage (up to 2V) the threshold potential shifted towards high voltage. This is because grid voltage also contributes for the reaction along applied voltage. Therefore, for these both voltage contribute to reaction and hence current increase with applied and grid voltage.

Table 4.2: Reaction starting voltage, over potential, slope and operating resistance of the cell for anode cathode ( $I_c$ ) at different fixed grid voltage

Fixed grid voltage( $V_g$ ) in volt	Reaction starting voltage ( $V_s$ ) in volt	Over potential in volt( $V_s-1.23$ )	Slope of the curve	Resistance(1/slope) in ohm
0.5	1.8	0.57	0.56	1.79
1	2	0.77	0.62	1.61
1.5	2	0.77	0.65	1.54
2	2	0.77	0.61	1.64
2.5	2	0.77	0.51	1.96
3	2.1	0.87	0.45	2.22
3.5	2.5	1.27	0.56	1.79
4	2.5	1.27	0.72	1.39

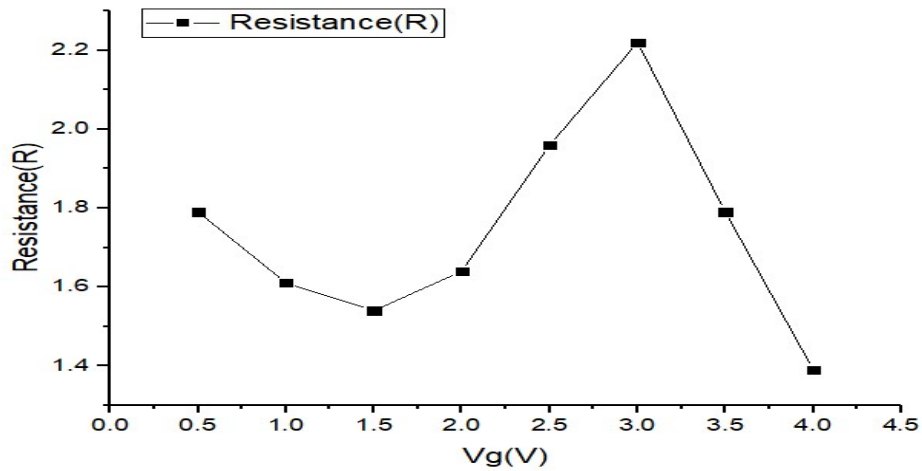


Figure 4.5: Graph showing variation of cell resistance (R) with grid voltage ( $V_g$ ) of Table 4.2

From above Figure 4.5 show that the variation of cell resistance (R) with grid voltage ( $V_g$ ). The plot for fixed grid voltage at  $V_g=0.5V$ , the resistance was observed 1.79ohm; at  $V_g=1.0V$ , the resistance was observed 1.61ohm; at  $V_g=1.5$ , the resistance was observed 1.54ohm and so on. The graph above in figure 4.5 shows with increasing in grid voltage cell resistance decrease with slope up to 1.5V and then cell resistance increases sharply with increasing grid voltage upto 3.0V and finally decrease sharply beyond 3.0V.

### 4.2.3 Effect of $V_g$ on $I_g$ verse $V_{ca}$ curve

Figure 4.6 shows that the curve of grid current ( $I_g$ ) with applied anode to cathode voltage ( $V_{ca}$ ) at different fixed grid voltages at 0.5V, 1.0V, 1.5V, 2.0V, 2.5V, 3.0V, 3.5V and 4.0V. When we increased the grid voltage up to  $V_g=0.5V$  to 1.5V then grid current ( $I_g$ ) is not observed. At  $V_g=2.0V$  the reaction starting voltage 1.6V then grid current decrease and applied voltage increase and similar nature for other fixed grid voltage is observed.

From graph, we obtained the  $V_{ca}$  is increases and  $I_g$  is decreases. The reaction starting voltage, over potential, slope and resistance is tabulated in 2<sup>nd</sup>, 3<sup>rd</sup>, 4<sup>th</sup> and 5<sup>th</sup> columns of table 4.3 respectively. The slope of the curve for different fixed grid voltage is determined by the linear fitting of curve.

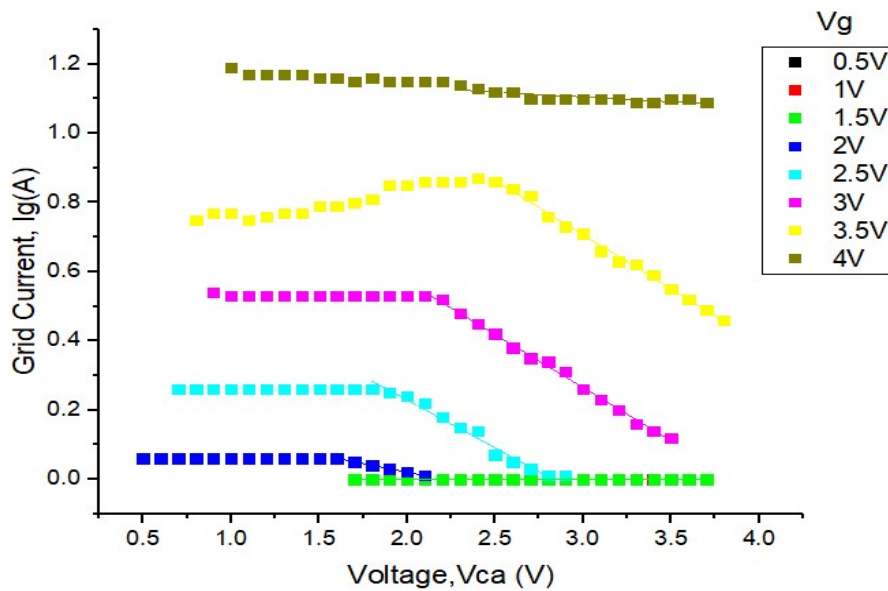


Figure 4.6: The variation of cathode current ( $I_c$ ) Verse applied voltage ( $V_{ca}$ ) for the cell with small windows size grid

In initial phase the applied voltage is used for threshold therefore current is constant and goes decreases as applied voltage increase because flow of electron is barrier by the gap (size of hole) of grid.

Table 4.3: Reaction starting voltage, over potential, slope and operating resistance of the cell for grid current at different fixed grid voltage

Fixed grid voltage( $V_g$ ) in volt	Reaction starting voltage ( $V_s$ ) in volt	Over potential in volt( $V_s-1.23$ )	Slope of the curve	Resistance(1/slope) in ohm
2	1.6	0.37	-0.1	10
2.5	2	0.77	-0.28	3.57
3	2.1	0.87	-0.31	3.23
3.5	2.5	1.27	-0.3	3.33
4	2.5	1.27	-0.307	3.26

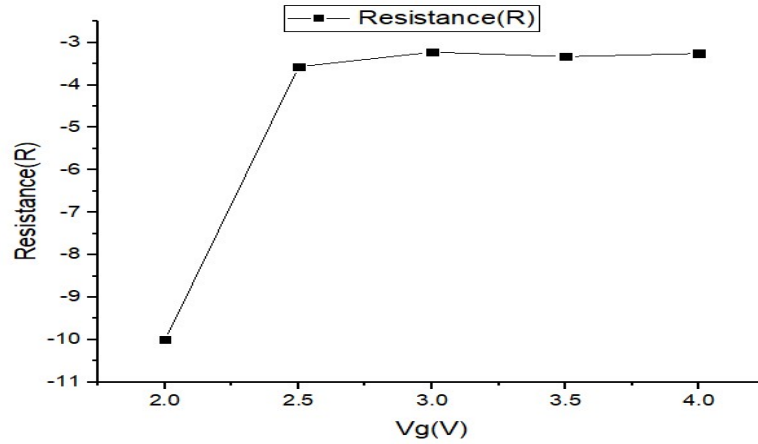


Figure 4.7: Graph showing variation of cell resistance (R) with grid voltage ( $V_g$ ) of Table 4.3

From above Figure 4.7 show that the variation of cell resistance (R) with grid voltage ( $V_g$ ). When we increase the grid voltage up to 1.5V then no resistance value is observed. Beyond the grid voltage 2.0V when grid voltage increase and resistance value increases.

#### 4.2.4 Effect of $V_g$ on Input power ( $P_{in}$ ) verse Cathode Current ( $I_c$ ) Curve

We have used the two power supply named  $P_1$  and  $P_2$  for our system and the potential across them is name by  $V_{ca}$  and  $V_g$  respectively. In order to check the maximum value of cathode current ( $I_c$ ) for the better performance of hydrogen production, we plotted hydrogen gas production current ( $I_c$ ) with input power ( $P_{in}$ ) at different fixed grid voltages, 0.5V, 1.0V, 1.5V, 2.0V, 2.5V, 3.0V, 3.5V and 4.0V. The Total input power due to  $P_1$  and  $P_2$  is calculated as,

$$\text{Total input power } (P_{in}) = I_a \times V_{ca} + I_g \times V_g$$

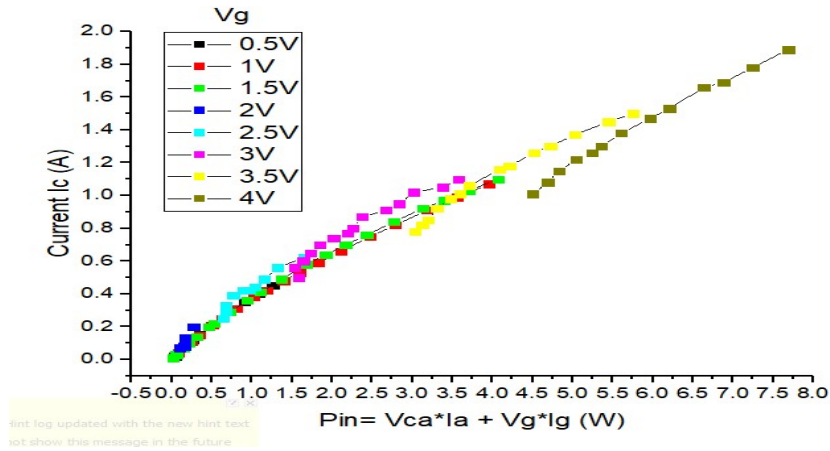


Figure 4.8: Plot of cathode current ( $I_c$ ) versus input power ( $P_{in}$ ) at different fixed grid voltage ( $V_g$ ) for common grid cell electrode configuration.

For each fixed grid voltage ( $V_g$ ),  $P_{in}$  is calculated using  $I_c$  and  $I_a$  values for different grid voltage using above relation of  $P_{in}$ . From Figure 4.8 shows the variation of cathode current ( $I_c$ ) in Ampere (A) with the variation of input power ( $P_{in}$ ) in watt at different fixed grid voltages. From graph, it is observed that the cathode current ( $I_c$ ) is increasing with increase in input power for all fixed grid voltages. From Figure 4.8 we also see that as Grid voltage increases and cathode current  $I_c$  is also increases with input power pin.

### 4.3 I-V Characteristics of Electrolyzer with Large Window Size Grid Electrode

Figure 4.1 shows the circuit diagram for power connection for the common cathode electrode configuration for alkaline water electrolyzer. Here steel mesh is used as grid electrode and placed in between anode electrode and cathode electrode. We used the large window size steel mesh for grid electrode. There are two jail are removed in row and column of steel mesh grid electrode. In this figure 4.1, negative terminal of power supply ( $P_1$ ) is connected to the cathode electrode ( $I_c$ ) and positive terminal of power supply ( $P_1$ ) is connected to the anode electrode.

Similarly, the positive terminal of power supply ( $P_2$ ) is connected to the grid electrode and negative terminal to the common junction of power supply ( $P_1$ ) and power supply ( $P_2$ ). The potential difference between anode electrode and cathode electrode is anode and cathode potential difference ( $V_{ca}$ ). Using 1 mole solution of (NaOH) electrolyte

solution and data has been recorded for fixed grid voltage. We have measured the anode current ( $I_a$ ), grid current ( $I_g$ ) and cathode current ( $I_c$ ) by varying  $V_{ca}$  for different fixed voltage ( $V_g$ ).

#### 4.3.1 Effect of $V_g$ on $I_a$ verse $V_{ca}$ Curve

Figure 4.9 shows that the curve of anode current ( $I_a$ ) with applied voltage ( $V_{ca}$ ) at different fixed grid voltages at 0.5V, 1.0V, 1.5V, 2.0V, 2.5V, 3.0V and 4.0V. From the graph, we find that, at grid voltage ( $V_g$ ) = 0.5V case, as applied voltage ( $V_{ca}$ ) is increased from 0 to 1.7 volts, no anode current is observed. Anode current ( $I_a$ ) appears to start when as applied voltage ( $V_{ca}$ ) is greater than 1.7V which indicates the starting voltage for water electrolysis. Beyond 1.7 V the anode current ( $I_a$ ) increases linearly.

From graph, we obtained as applied voltage ( $V_{ca}$ ) increases and anode current ( $I_a$ ) also increases linearly. Theoretical water splits to start at 1.23V, which is considered as threshold voltage for water electrolysis. In our case, at  $V_g=0.5V$ , the reaction starting voltage is found to be 1.8V and over potential is 0.57V. The reaction starting voltage, over potential, slope and cell resistance is tabulated in 2<sup>nd</sup>, 3<sup>rd</sup>, 4<sup>th</sup> and 5<sup>th</sup> columns of table 4.4 respectively. The slope of the curve for different fixed grid voltages are determined by the linear fitting of curve.

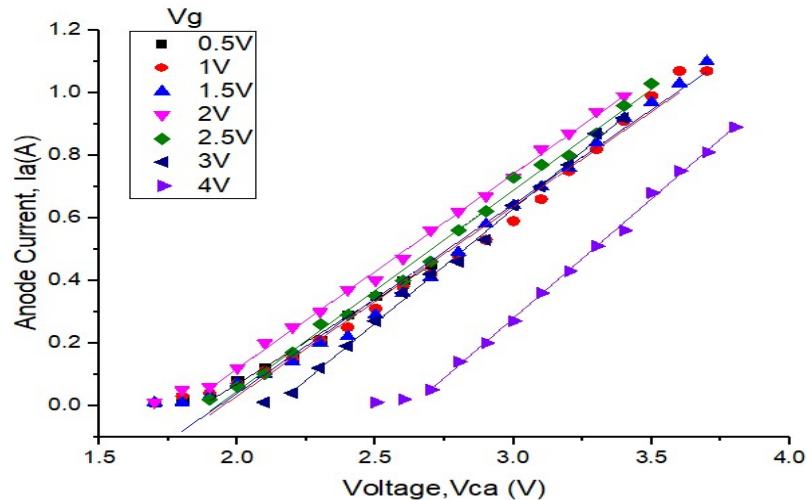


Figure 4.9: the variation of anode current ( $I_a$ ) Verse applied voltage ( $V_{ca}$ ) for the cell with large window size grid.

Table 4.4: Reaction starting voltage, over potential, slope and operating resistance of the cell for anode current at different fixed grid voltage

Fixed grid voltage( $V_g$ ) in volt	Reaction starting voltage ( $V_s$ ) in volt	Over potential in volt( $V_s-1.23$ )	Slope of the curve	Resistance(1/slope) in ohm
0.5	1.8	0.57	0.54	1.85
1	2	0.77	0.62	1.61
1.5	2	0.77	0.63	1.59
2	2	0.77	0.62	1.57
2.5	2	0.77	0.64	1.56
3	2.2	0.97	0.73	1.37
4	2.7	1.47	0.75	1.33

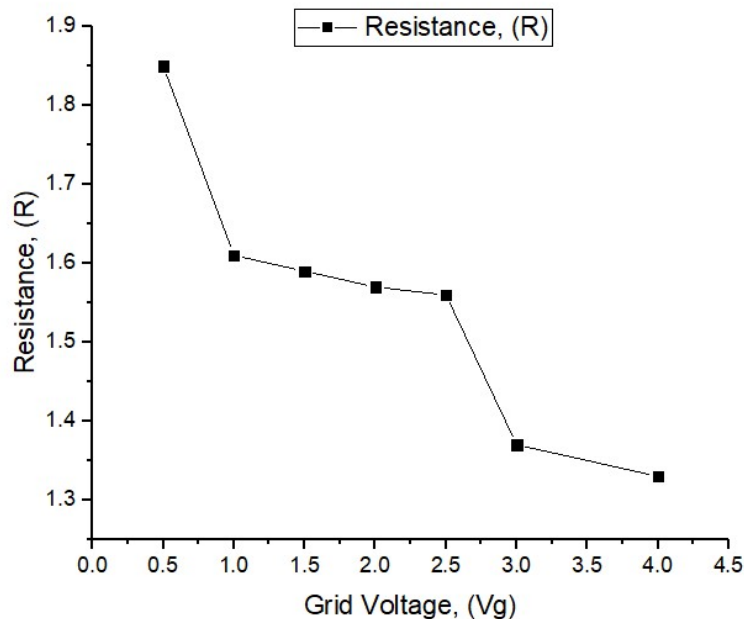


Figure 4.10: Graph showing variation of cell resistance (R) with grid voltage ( $V_g$ ) of Table 4.4

From above Figure 4.10 show that the variation of cell resistance (R) with grid voltage ( $V_g$ ). When we plot at  $V_g=0.5V$  then we found the resistance value is 1.85 ohm. Again we plot at  $V_g=1.0V$  then we found resistance value is 1.61 and so on. Similarly we plot at  $V_g=4.0$  then we found the resistance value is 1.33 ohm. Thus, the grid voltage ( $V_g$ ) increases then the resistance value is decreases.



### 4.3.2 Effect of $V_g$ on $I_c$ Verse $V_{ca}$ Curve

Figure 4.11 shows that the curve of cathode current ( $I_c$ ) with applied voltage ( $V_{ca}$ ) at different fixed grid voltages at 0.5V, 1.0V, 1.5V, 2.0V, 2.5V, 3.0V and 4.0V. From graph, At  $V_g=0.5V$  the reaction starting voltage above the 1.8 volt then we observed  $V_{ca}$  is increases and  $I_c$  is also increases linearly. At  $V_g=2.0V$  the cathode current ( $I_c=0.1A$ ) and applied voltage ( $V_{ca}$ ) are constant up to 1.9V then the reaction starting voltage above 2V then cathode current increases and applied voltage increases linearly.

At  $V_g=2.5V$  the cathode current ( $I_c= 0.2A$ ) and applied voltage ( $V_{ca}$ ) are constant up to 1.9V then the reaction starting voltage above 2V then cathode current increases and applied voltage increases linearly and so on. Similarly At  $V_g=4.0V$  the cathode current ( $I_c= 1.0A$ ) and Applied voltage  $V_{ca}$  are constant up to 3.0V then the reaction starting voltage above 3.0V then cathode current ( $I_c$ ) increase and applied voltages increases linearly. The reaction starting voltage, over potential, slope and resistance is tabulated in 2<sup>nd</sup>, 3<sup>rd</sup>, 4<sup>th</sup> and 5<sup>th</sup> columns of table 4.5 respectively. The slope of the curve for different fixed grid voltage is determined by the linear fitting of curve

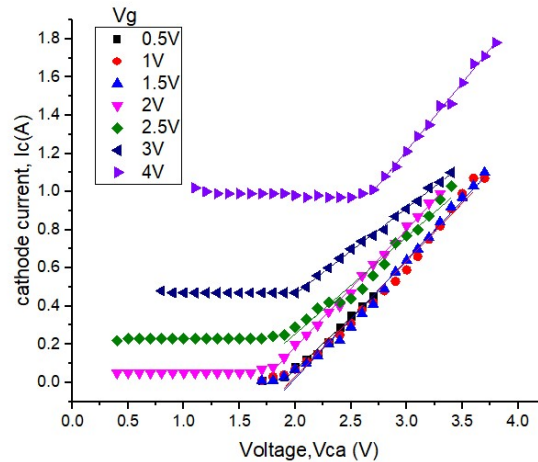


Figure 4.11: the variation of cathode current ( $I_c$ ) Verse applied voltage ( $V_{ca}$ ) for the cell with large window grid.

The cathode current is minimum or tends to zero because the threshold potential required for the reaction is 1.23 and grid voltage can't cross this threshold potential although grid

voltage increase up to 2V. This is because impurities and concentration of electrolyte and experimental arrangement. With increasing grid and applied voltage (upto2V) the threshold potential shifted towards high voltage. This is because grid voltages also contribute for the reaction along applied voltage. Therefore, for these both voltage contribute to reaction and hence current increase with applied and grid voltage.

Table 4.5: Reaction starting voltage, over potential, slope and operating resistance of the cell for anode cathode ( $I_c$ ) at different fixed grid voltage

Fixed grid voltage( $V_g$ ) in volt	Reaction starting voltage ( $V_s$ ) in volt	Over potential in volt( $V_s-1.23$ )	Slope of the curve	Resistance(1/slope) in ohm
0.5	1.8	0.57	0.56	1.79
1	2	0.77	0.62	1.61
1.5	2	0.77	0.62	1.61
2	2	0.77	0.62	1.61
2.5	2	0.77	0.52	1.92
3	2	0.77	0.45	2.15
4	3	1.77	0.66	1.52

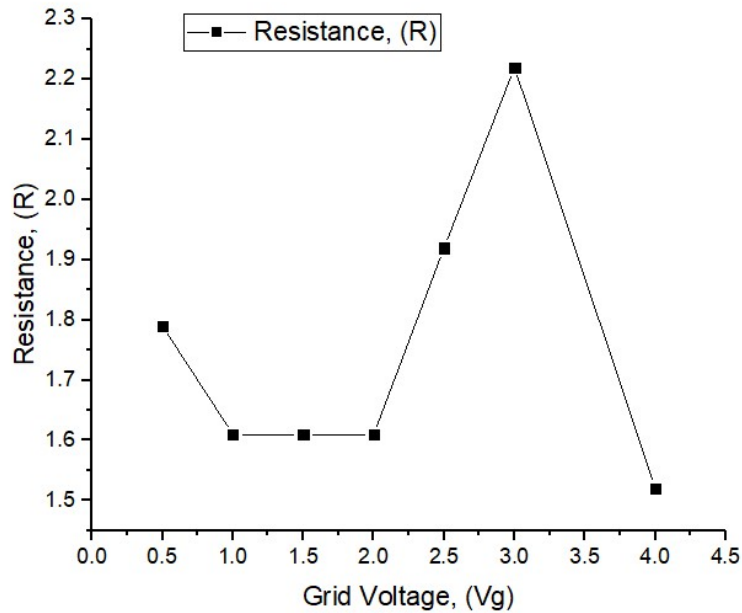


Figure4.12: Graph showing variation of cell resistance (R) with grid voltage ( $V_g$ ) of

Table 4.5

From above Figure 4.12 show that the variation of cell resistance (R) with grid voltage ( $V_g$ ). When we plot at  $V_g=0.5V$  then we found the resistance value is 1.79 ohm. We plot at  $V_g=1.0V$  to 2.0V then we found same resistance value is 1.61. Again we have increased the grid voltages from  $V_g=2.0V$  to 3.0V then the resistance are increases. Similarly when we have increased the grid voltages  $V_g=3.0V$  to 4.0V then finally resistance decreases.

### 4.3.3 Effect of $V_g$ on $I_g$ verse $V_{ca}$ Curve

Figure 4.13 shows that the curve of grid current ( $I_g$ ) with applied voltage ( $V_{ca}$ ) at different fixed grid voltages at 0.5V, 1.0V, 1.5V, 2.0V, 2.5V, 3.0V, and 4.0V. when we increased the grid voltage up to  $V_g=0.5V$  to 1.5V then grid current ( $I_g$ ) is not observed. At  $V_g=2.0V$  the reaction starting voltage 1.5V then grid current decrease and applied voltage increase and so on.

Similarly at  $V_g=4.0V$  the reaction starting voltage 0.8V then grid current decrease and applied voltage increase. From graph, we obtained the  $V_{ca}$  is increases and  $I_g$  is decreases. The reaction starting voltage, over potential, slope and resistance is tabulated in 2<sup>nd</sup>, 3<sup>rd</sup>, 4<sup>th</sup> and 5<sup>th</sup> columns of table 4.6 respectively. The slope of the curve for different fixed grid voltage is determined by the linear fitting of curve.

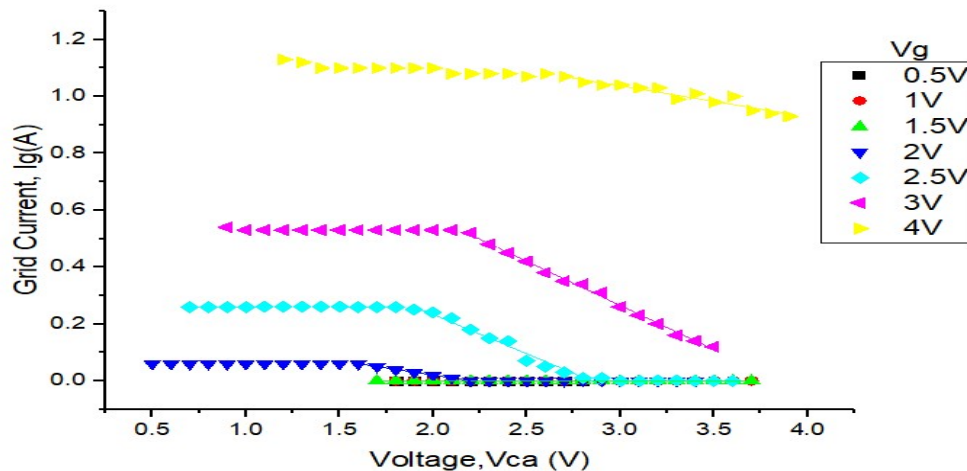


Figure 4.13: Variation of cathode current ( $I_c$ ) Verse applied voltage ( $V_{ca}$ ) for the cell with large windows size grid

In initial phase the applied voltage is used for threshold therefore current is constant and goes decreases as applied voltage increase because flow of electron is barrier by the gap (size of hole) of grid.

Table4.6: Reaction starting voltage, over potential, slope and operating resistance of the cell for grid current at different fixed grid voltage

Fixed grid voltage( $V_g$ ) in volt	Reaction starting voltage ( $V_s$ ) in volt	Over potential in volt( $V_s-1.23$ )	Slope of the curve	Resistance(1/slope) in ohm
2	1.5	0.27	-0.1	10
2.5	1.8	0.57	-0.23	4.3
3	2	0.77	-0.31	3.2
4	2.5	1.27	-0.35	2.86

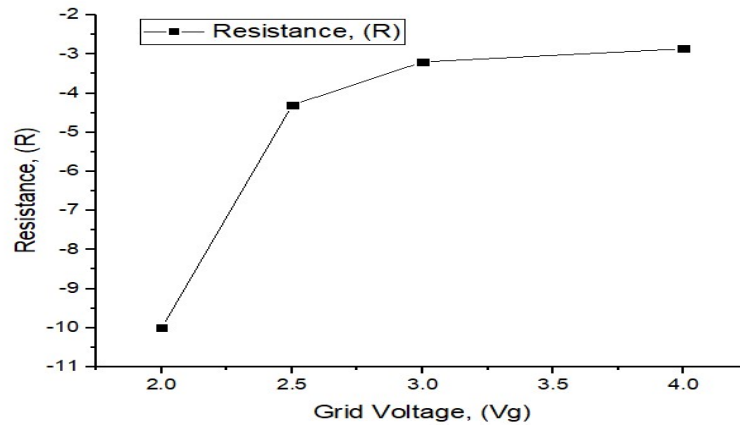


Figure 4.14: Graph showing variation of cell resistance (R) with grid voltage ( $V_g$ ) of Table 4.6

From above Figure 4.6 show that the variation of cell resistance (R) with grid voltage ( $V_g$ ). When we increase the grid voltage up to 1.5V then no resistance value is observed. Beyond the grid voltage 2.0V when grid voltage increase and resistance value increases.

#### 4.3.4 Effect of $V_{ca}$ on Input Power ( $P_{in}$ ) verse Cathode Current ( $I_c$ )

We have used the two power named  $P_1$  and  $P_2$  for our system and the potential across them is name by  $V_{ca}$  and  $V_g$  respectively. In order to check the maximum value of cathode current ( $I_c$ ) for the better performance of hydrogen production, we plotted hydrogen gas production current ( $I_c$ ) with input power ( $P_{in}$ ) at different fixed grid

voltages, 0.5V, 1.0V, 1.5V, 2.0V, 2.5V, 3.0V and 4.0V. The Total input power due to  $P_1$  and  $P_2$  is calculated as,

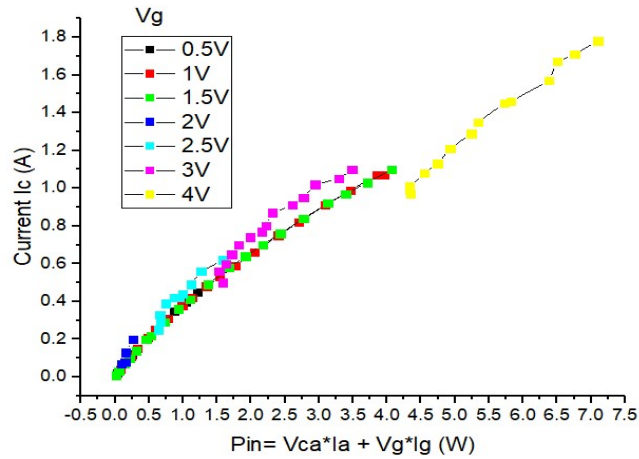


Figure 4.15 Plot of cathode current ( $I_c$ ) verse input power ( $P_{in}$ ) at different fixed grid voltage ( $V_g$ ) for common grid cell electrode configuration.

For each fixed grid voltage ( $V_g$ ),  $P_{in}$  is calculated using  $I_c$  and  $I_a$  values for different grid voltage with the help of  $P_{in}$  relation described above. From Figure 4.15 shows the variation of cathode current ( $I_c$ ) in Ampere (A) with the variation of input power ( $P_{in}$ ) in watt at different fixed grid voltages. From graph, it is observed that the cathode current ( $I_c$ ) is increasing with increase in input power for all fixed grid voltages. From Figure 4.15 we also see that as Grid voltage increases and cathode current  $I_c$  is also increases with input power  $P_{in}$ .

#### 4.4. The Comparison Graph between Small & Large Window Size Grid Electrode at Grid Voltage $V_g=3.0V$

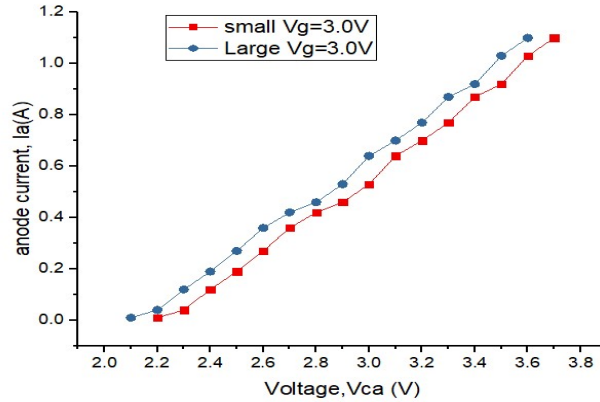


Figure 4.16: The comparison graph between small & large window size grid electrode at grid voltage  $V_g=3.0V$ .

From figure 4.16 shows that the comparison graph between small and large window size grid electrode at  $V_g=3.0V$ . When we increase the surface area of grid electrode then increase the hydrogen production rate. This is because large surface area goes to contact with large number of electrolyte molecules and the production of hydrogen depend up on this contact i.e. larger surface area has large number of reaction. Therefore the productions of hydrogen gas depend upon the surface area of grid.

#### 4.5. Comparison Graph of experimental and Theoretical ( $H_2$ ) Production rate verse Current

Table 4.7: Hydrogen and Oxygen Production rate

Current(A)	Experimental $H_2$ production	Theoretical $H_2$ Productions
0.2	1.92	1.39
0.4	3.53	2.78
0.6	5.11	4.18
0.8	6.45	5.67
1.0	8.51	6.96

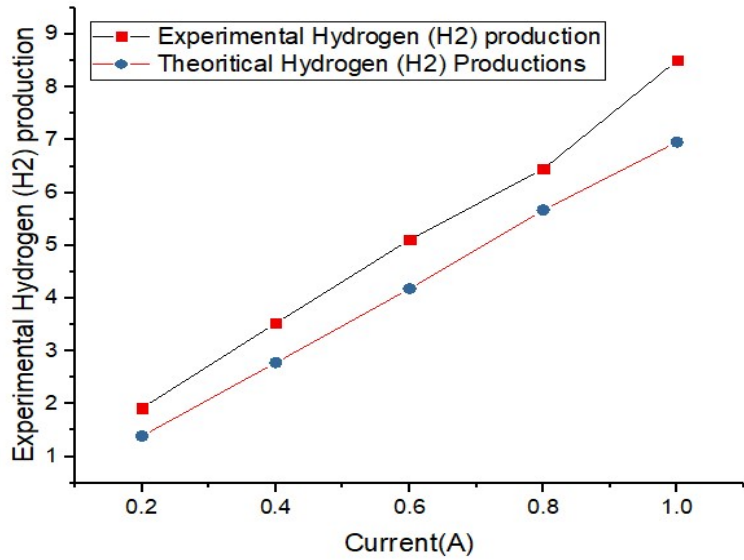


Figure 4.17: Plot of hydrogen production rate versus current at different fixed grid voltage ( $V_g$ ) for common grid cell electrode configuration.

When the current increases and the hydrogen production rate increases linearly similarly, when current is decreased the hydrogen production rate decreases and vice versa.

#### 4.6. Comparison of Pin with cathode current at constant grid voltage

From figure 4.18, it is concluded that with increasing the surface area of grid electrode then the production of hydrogen increases and hence input power increases.

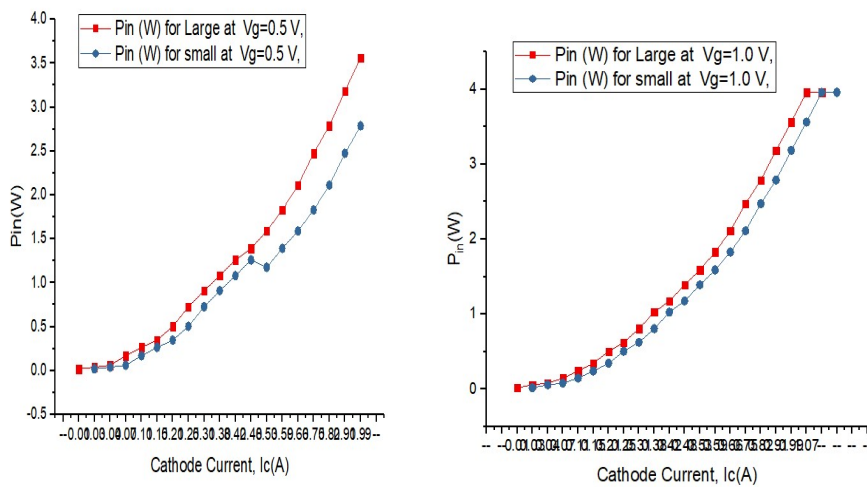


Figure 4.18: Input Power vs cathode current with large and small windows sizes

## CHAPTER FIVE: CONCLUSION

### 5.1 Conclusion

Electrolysis is the simplest way for hydrogen production and electrical energy production. I have tried my best use the different sizes of grid electrode for the study of hydrogen Production by water electrolysis method. It is very useful in our daily life as well as long life. The efficiency of the hydrogen production through this experiment setup is about 68%. This efficiency was calculated with the help of electrodes current made up of steels. The new three electrode system for water electrolysis was successfully constructed. The over potential was observed to increase with increase in grid voltage. The slope of I-V curve was observed to increase with increase in grid voltage indicating inclusion of grid voltage may lead to increase hydrogen in production rate. The increase with windows size the production rate of hydrogen production rate increase. The production of hydrogen increase with surface area of grid and hence power increases.

With increase the surface area of grid electrode then increase the hydrogen production rate. This is because large surface area goes to contact with large number of electrolyte molecules and the production of hydrogen depend up on this contact i.e. larger surface area has large number of reaction. Therefore the productions of hydrogen gas depend upon the surface area of grid. Grid voltage increases and cathode current  $I_c$  is also increases with input power  $p_{in}$ . Thus, in general one can say with increasing the grid voltage cell resistance decrease. The resistance of cell decrease sharply in between 0.5V to 1.0V with grid voltage while seen almost constant beyond 3.5V.

### 5.2 Future work

This work may help to compare the hydrogen production with other phenomena and factors with various components used in this experiment. The production of hydrogen with this experiment is cheap and ecofriendly. Since the storage of hydrogen is one of the major problems therefore one can used this system to generate the energy parallel. The generated hydrogen from this system can used in hydrogen fuel winch is emerging technology. The study of surface area of grid help to design the electrodes which increase the production of hydrogen.



## References

- A.F.M and M. S. (2011). Experimental Investigation of the Operating Parameters Affecting Hydrogen Production Process through Alkaline Water Electrolysis. *International Journal of Thermal & Environmental Engineering*, 2, 113-116.
- A. Konopka and D. Gregory. (1975). Hydrogen Production by Electrolysis: Present and Future,” presented at 10th Intersociety Energy Conversion Engineering Conference, IEEE Cat. No. 75CHO 983-7 TAB.
- A. McWilliams. (2019). Hydrogen as a Chemical Constituent and as an Energy Source, Available:<https://www.bccresearch.com/market-research/chemicals/hydrogen-as-a-chemical-constituent-and-as-an-energy-source-chm031d.html>.
- Badwal, S.P.S.Giddey, S. and Ciachi, F. T. (2006), “Hydrogen and oxygen generation with polymer electrolyte.
- Bocca, C.; Barbucci, A.; Cerisola, G. (1998). *Int. J. Hydrogen Energy*, 23, 247.
- Bouazizi Nabil, B. R. (2014). Hydrogen Production by Electrolysis of Water, *Global Journal of Science Frontier Research*, 2249-4626.
- Bowen, C. T. Davis, H. J. Henshaw, B. F. Lachance, R. Leroy, R. L. Renaud, R.(1984) *Int. J. Hydrogen Energy*, 9, 59.
- De Levie, R. (1999). *J. Electroanal. Chem.*, 476, 92.
- Divisek, J. Mergel, J. Schmitz, H. (1990), *Int. J. Hydrogen Energy*, 15, 105.
- Diogo M. F. Santos, C. A. (2013). Hydrogen production by alkaline water electrolysis. *Quim. Nova*, 1176-1193.
- Dunnill, G. P. (2015). Water Splitting Test Cell for Renewable Energy Storage as Hydrogen Gas. *J. of fundamental of Renewable Energy and Applications*, 5.

- Eedulakanti, S. R. (2019). Ultra-sonication assisted thermal exfoliation of graphene-tin oxide nanocomposite material for super capacitor. *Materials Science for Energy Technologies*, 372-376.
- Ganley, J.C. (2009), High temperature and pressure alkaline electrolysis, *International Journal of Hydrogen Energy*, 34(5), 3604–3611.
- Hickner, M. A. Ghassemi, H. Kim, Y. S. Einsla, B. R. McGrath, J. E. (2004). *Chem. Rev.*, 104, 4587.
- Hydrogen Council. (2017), Hydrogen scaling up - A sustainable pathway for the global energy transition, Available:<http://hydrogencouncil.com/wp-content/uploads/2017/11/Hydrogen-scaling-up-Hydrogen-Council.pdf>.
- H.P., M., & A.K., G. (1979). *Solar Energy material*, 411.
- IRENA. (2018). *Hydrogen from renewable power: Technology outlook for the energy transition*, Abu Dhabi.
- J.A. Turner, (2004). Sustainable Hydrogen Production, *Science*, 305(5686), 972-974.
- K., Z., & D, Z. (2010). Recent Progress in alkaline water electrolysis for hydrogen production and its applications. *J. of Progress in Energy and Combustion Science*, 10, 307-326.
- Kandah, M.I. (2014). Enhancement of Water Electrolyzer Efficiency, *Journal of Energy Technologies and Policy*, 4(11), 1-2,
- Kreuter, W. Hofmann, H. (1998). *Int. J. Hydrogen Energy* 1998, 23, 661.
- Lin, M.Y. (2012). The effect of magnetic force on hydrogen production efficiency. *International journal of hydrogen energy*, 1311-1320.
- M. Hurskainen, J. Kärki, (2018), VTT internal research report.

Mansouri, K., et al. (2001), Anodic dissolution of pure aluminum during electro coagulation process: influence of supporting electrolyte initial pH, and current density, *Industrial and Engineering Chemistry Research* 50 (23), 13362–13372.

Munoz, L.D.S. et al., (2010), Hydrogen production by electrolysis of a phosphate solution on a stainless steel cathode. *International Journal of Hydrogen Energy*, 8561-8568.

M., R., & K.F, K. (1989). *Internal Journal of Hydrogen Energy*, 545-549.

M.M, R., k, M., H, N., & M, D. (2015). *Hydrogen Production System. IJEAT*, 4.

Nagai, N. et al., (2003), Existence of optimum space between electrodes on hydrogen production by water electrolysis, *International Journal of Hydrogen Energy*, 28(1), 35–41.

Kauranen, P. et al., (2013). *Vetytiekartta - vetyenergianmahdollisuudetSuomessa*, Available: <https://www.vtt.fi/inf/julkaisut/muut/2013/VTT-R-02257-13.pdf>.

Petrov, Y. et al. (2011). Hydrogen evolution on nickel electrode in synthetic tap water alkaline solution, *International Journal of Hydrogen Energy*, 36(20), 12715-12724.

Pletcher, D. Walsh, F. C. (1990). *Industrial electrochemistry*, 2<sup>nd</sup>ed., Blackie Academic & Professional: London.

P.Millet, (2010). PEM water electrolyzer: From electro catalysis to stack development. *Internal Journal of Hydrogen Energy*, 7, 5043-5052.

Petrov, Y. (2011). Hydrogen evolution of nickel electrode in synthetic tap water-alkaline solution. *International Journal of Hydrogen Energy*, 8, 15-24.

Prinith, N. (2019). Surfactant modified electrochemical sensor for determination of Anthrone – A cyclic voltammetry, *Materials Science for Energy Technologies*, 10, 408-416.

Rieger, P. H. (1987). *Electrochemistry*, 1<sup>st</sup>ed., Prentice-Hall: New Jersey.

- Rosa, V. M.; Santos, M. B. F.; Da Silva, E. P. (1995). *Int. J. Hydrogen Energy*, 20, 697.
- Ryton®, (2006). PPS - Chevron Phillips Chemical Company LLC. Available: [www.cpchem.com/enu/ryton\\_pps.asp](http://www.cpchem.com/enu/ryton_pps.asp),
- Rosen, M. A. (2008). The Prospects for Renewable Energy through Hydrogen Energy Systems. *Journal of Power and Energy Engineering*, 13, 4013-4029.
- Sequeira, C. A. C.; Santos, D. M. F. (2010). *Ciência & Tecnologia dos Materiais*, 22, 76.
- Santos, D. M. (2013). Hydrogen production by alkaline water electrolysis. *Quím. Nova*, 8, 12-15.
- Sun, C.W. and Hsiau, S.S, (2018), Effect of Electrolyte Concentration Difference on Hydrogen Production during PEM Electrolysis, *Journal of Electrochemical Science and Technology*, 9(2), 99-108.
- Valladares, M.R. (2017), Global trends and outlook for hydrogen, Available: <http://ieahydrogen.org/pdfs/Global-Outlook-and-Trends-for-Hydrogen-Dec2017-WEB.aspx>.
- V.M. Nikolic, G. T. (2010). *International Journal of Hydrogen Energy*, 35.
- Voitic, G. (2018). Hydrogen Production. *Fuel Cells and Hydrogen*, 215-241.
- W.P., S. (2004). Hydrogen Energy and Photo electrolysis of water, 67-73.
- Walch, G. (2014). Correlation between hydrogen production rate, current, and electrode over potential in a solid oxide electrolysis cell with La<sub>0.6</sub>Sr<sub>0.4</sub>FeO<sub>3-δ</sub> thin-film cathode. *Monat sheftefürChemie - Chemical Monthly*, 1055-1061.
- Wendt, H. Kreysa, G. (1999). *Electrochemical engineering*, 1st ed., SpringerVerlag: Berlin, Heidelberg.
- W. Kincaide, (1978). *Alkaline Electrolysis: Past, Present and Future*, presented at Hydrogen for Energy Distribution, Institute of Gas Technology, 1978.

## Appendix

### Power supply calibration curve

The graph between standard multimeter voltage vs. power supply one reading

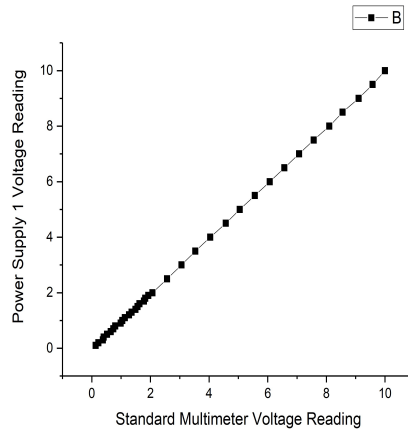


Figure A1: Power Supply 1 Vs Standard Multimeter voltage

Figure A1 shows that the graph between power supply one calibrated voltage reading and standard multimeter calibrated voltage reading. It is linear nature and power supply one provides corrected data. When the data measured both multimeter and power supply one gives the identical reading and the nature of graph is linear

The graph between standard multimeter voltages vs. power supply two reading

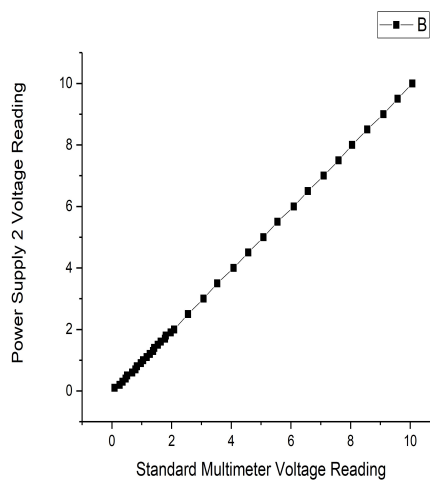


Figure A2: Power Supply 2 Vs Standard Multimeter voltage

Figure A2 shows that the graph between powers supplies two calibrated voltage reading and standard multimeter calibrated voltage reading. It is linear nature and power supply two provides corrected data. When the data measured both multimeter and power supply two gives the identical reading and the nature of graph is linear.